

An overview on the removal of synthetic dyes from water by electrochemical advanced oxidation processes.

P Nidheesh, Minghua Zhou, Mehmet A. Oturan

► To cite this version:

P Nidheesh, Minghua Zhou, Mehmet A. Oturan. An overview on the removal of synthetic dyes from water by electrochemical advanced oxidation processes.. *Chemosphere*, Elsevier, 2018, 197 (210-227.), 10.1016/j.chemosphere.2017.12.195 . hal-01721053

HAL Id: hal-01721053

<https://hal-upec-upem.archives-ouvertes.fr/hal-01721053>

Submitted on 1 Mar 2018

HAL is a multi-disciplinary open access archive for the deposit and dissemination of scientific research documents, whether they are published or not. The documents may come from teaching and research institutions in France or abroad, or from public or private research centers.

L'archive ouverte pluridisciplinaire **HAL**, est destinée au dépôt et à la diffusion de documents scientifiques de niveau recherche, publiés ou non, émanant des établissements d'enseignement et de recherche français ou étrangers, des laboratoires publics ou privés.

An overview on the removal of synthetic dyes from water by electrochemical advanced oxidation processes

P. V. Nidheesh¹, Minghua Zhou², Mehmet A. Oturan^{3,*}

¹ CSIR-National Environmental Engineering Research Institute, Nagpur, Maharashtra, India

² Key Laboratory of Pollution Process and Environmental Criteria, Ministry of Education,
Tianjin Key Laboratory of Urban Ecology Environmental Remediation and Pollution
Control, College of Environmental Science and Engineering, Nankai University, Tianjin
300350, P. R. China.

³ Université Paris-Est, Laboratoire Géomatériaux et Environnement, (LGE), , EA 4508,
UPEM, 5 Bd Descartes, 77454 Marne-la-Vallée Cedex 2, France

Paper submitted for publication in SI: EAOPs-POPs, Chemosphere

*Corresponding author:

Email: Mehmet.Oturan@univ-paris-est.fr (Mehmet A. Oturan)

Tel.: +33 (0)1 49 32 90 65

1 **Abstract**

2 Wastewater containing dyes are one of the major threats to our environment. Conventional
3 methods are insufficient for the removal of these persistent organic pollutants. Recently much
4 attention has been received for the oxidative removal of various organic pollutants by
5 electrochemically generated hydroxyl radical. This review article aims to provide the recent
6 trends in the field of various electrochemical advanced oxidation processes (EAOPs) used for
7 removing dyes from water medium. The characteristics, fundamentals and recent advances in
8 each processes namely anodic oxidation, electro-Fenton, peroxicoagulation, fered Fenton,
9 anodic Fenton, photoelectro-Fenton, sonoelectro-Fenton, bioelectro-Fenton etc. have been
10 examined in detail. These processes have great potential to destroy persistent organic
11 pollutants in aqueous medium and most of the studies reported complete removal of dyes
12 from water. The great capacity of these processes indicates that EAOPs constitute a
13 promising technology for the treatment of the dye contaminated effluents.

14

15 **Keywords:** Dye removal, Electrochemical advanced oxidation, Decolorization,
16 Mineralization, Hydroxyl radicals, Wastewater treatment

17

18 **1. Introduction**

19 Water pollution due to various industrial effluents is a global environmental problem.
20 Due to the rapid industrialization, the use of coloring chemicals like dyes also increases day
21 by day. Overall, 40,000 dyes and pigments with more than 7,000 different chemical
22 structures have been reported recently (Demirbas, 2009). Production of dyestuff and
23 pigments annually across the world is more than 700,000 tonnes and in India itself it is close
24 to 80,000 tonnes (Mathur et al., 2005; Gong et al., 2007; Mane et al., 2007). Among this
25 10,000 different types of dyes and pigments are being manufactured annually across the
26 world (Ponnusami et al., 2008). These dyes are chemically, photolytically and biologically
27 highly stable and are highly persistent in nature (Suteu and Bilba, 2005). Various industries
28 like textile, leather, food, cosmetic, paper, pharmaceutical etc. are using variety of synthetic
29 dyes. Among these industries, textile industries are the largest consumer of dyeing stuffs and
30 pigments and produces large amount effluents after dyeing process. For example, 1.5 million
31 liters per day of effluent are discharging into natural water bodies from an average mill
32 producing 60×10^4 m of fabric (COINDS, 2000). This wastewater contains various kinds of
33 pollutants apart from dyes and most of them are hazardous. Depending on the textile
34 processes, effluents generated from the industry contains various types of solvents, salts,
35 detergents etc. apart from many types of dyes (Barredo-Damas et al., 2006). Typical
36 characteristics of the effluent generated from textile industries are given in Table 1. Among
37 these contaminants, removal of dyes from the wastewater needs to be a special attention.

38 The effluents containing dyes are one of the major threats to environment. Even in low
39 concentrations, the dyes are highly visible (esthetic pollution) and affect the aquatic life and
40 food chain (chemical pollution) (Namasivayam and Kavitha, 2002; Malik, 2003). However,
41 the average concentration of dyes in a textile wastewater is around 300 mg L^{-1} (Couto, 2009).
42 Disposal of this highly colored wastewater into natural water bodies hamper light penetration,

43 distress biological process in the water medium and provide an aesthetically displeasing
44 appearance (Arivoli et al., 2009). Reduced light penetration with the introduction of colored
45 wastewater reduces the photosynthetic activity within the water body and this also affect the
46 symbiotic process (Ju et al., 2008).

47 **Table 1** Characteristics of textile wastewater. Reprinted with permission from Sandya et al.
48 (2008), Copyright 2007, Elsevier.

| Parameters | Concentration |
|---|---------------|
| Solution pH | 9.5-12.5 |
| Total Suspended Solids (mg L ⁻¹) | 60-416 |
| Total Dissolved Solids (mg L ⁻¹) | 4500-12800 |
| Total Organic Carbon (mg L ⁻¹) | 26390-73190 |
| Biochemical Oxygen Demand (mg L ⁻¹) | 25-433 |
| Chemical Oxygen Demand (mg L ⁻¹) | 1835-3828 |
| Aromatic Amines (mg L ⁻¹) | 20-75 |
| Ammonia (mg L ⁻¹) | 2-3 |
| Chloride (mg L ⁻¹) | 1200-1375 |
| Sulphate (mg L ⁻¹) | 700-2400 |

49
50 The hazardous, toxic and carcinogenic natures of dyes are also well known.
51 Physiological disorders in aquatic organisms happen by the consumption of dyes in textile
52 effluents via food chain (Karthikeyan et al., 2006). Some of the azo dyes are responsible for
53 causing bladder cancer in humans and chromosomal aberration in mammalian cells
54 (Mendevedev, 1988; Percy et. al., 1989). Cytotoxicity of reactive dyes (three
55 monochlorotriazinyl dyes: yellow, red and blue with different concentrations) using human
56 keratinocyte HaCaT cells in vitro was investigated by Klemola et al. (2007) and the mean
57 inhibitory concentration values after 72 h of exposure was measured as 237 µg mL⁻¹ for
58 yellow dye, 155 µg mL⁻¹ for red dye and 278 µg mL⁻¹ for blue dye. Similarly, spermatozoa

59 motility inhibition test of these dyes showed the mean inhibitory concentration values after
60 24 h of exposure as $135 \mu\text{g mL}^{-1}$ for yellow dye, $\mu\text{g mL}^{-1}$ for red dye and $127 \mu\text{g mL}^{-1}$ for
61 blue dye (Klemola et al., 2006). Frame-shift mutation and base pair substitution in
62 Salmonella in the presence of CI disperse blue was observed by Umbuzeiro et al. (2005).
63 Experimental investigations of Bae and Freeman (2007) reported that C.I. Direct Blue 218 is
64 very toxic to daphnids. The 50% of mortality of daphnids was observed for concentrations of
65 $1\text{-}10 \text{ mg L}^{-1}$ of C.I. Direct Blue 218 after 48 h. Impact of textile effluents on a proteinous
66 edible fresh water fish Mastacembelus Armatus was examined by Karthikeyan et al. (2006)
67 and they observed a decrease in Na^+ and Cl^- concentrations and increase in K^+ , Mg^{2+} and
68 Ca^{2+} concentrations after 35 d of Acid Blue 92 exposure. The toxicity of the textile dye
69 industry effluent on freshwater female crab, *Spiralothelphusa hydrodroma* was investigated
70 by Sekar et al. (2009). The authors observed a decrease in protein, carbohydrate and lipid
71 contents in ovary, spermatheca, muscle, hepatopancreas, gill, brain, thoracic ganglia and
72 eyestalks at 30 d of sublethal (69.66 ppm) concentration of textile dye industry effluent
73 exposure. Mathur et al. (2005) tested the mutagenic activity of seven dyes by Ames assay,
74 using strain TA 100 of Salmonella typhimurium and reported that except violet dye, all are
75 mutagenic. Among these mutagenic dyes, Congo red and royal blue dyes are moderately
76 mutagenic while bordeaux is highly mutagenic or extremely mutagenic. Similarly, effect of
77 malachite green on immune and reproductive systems was observed by Srivastava et al.
78 (2004). The authors also observed the potential genotoxic and carcinogenic nature of the
79 mentioned basic dye.

80 These non-exhaustive examples highlight how much the presence of the dyes in water
81 is harmful to the aquatic environment. Therefore, removal of dyes from aqueous medium is
82 an important environmental issue in the environmental safety point of view.

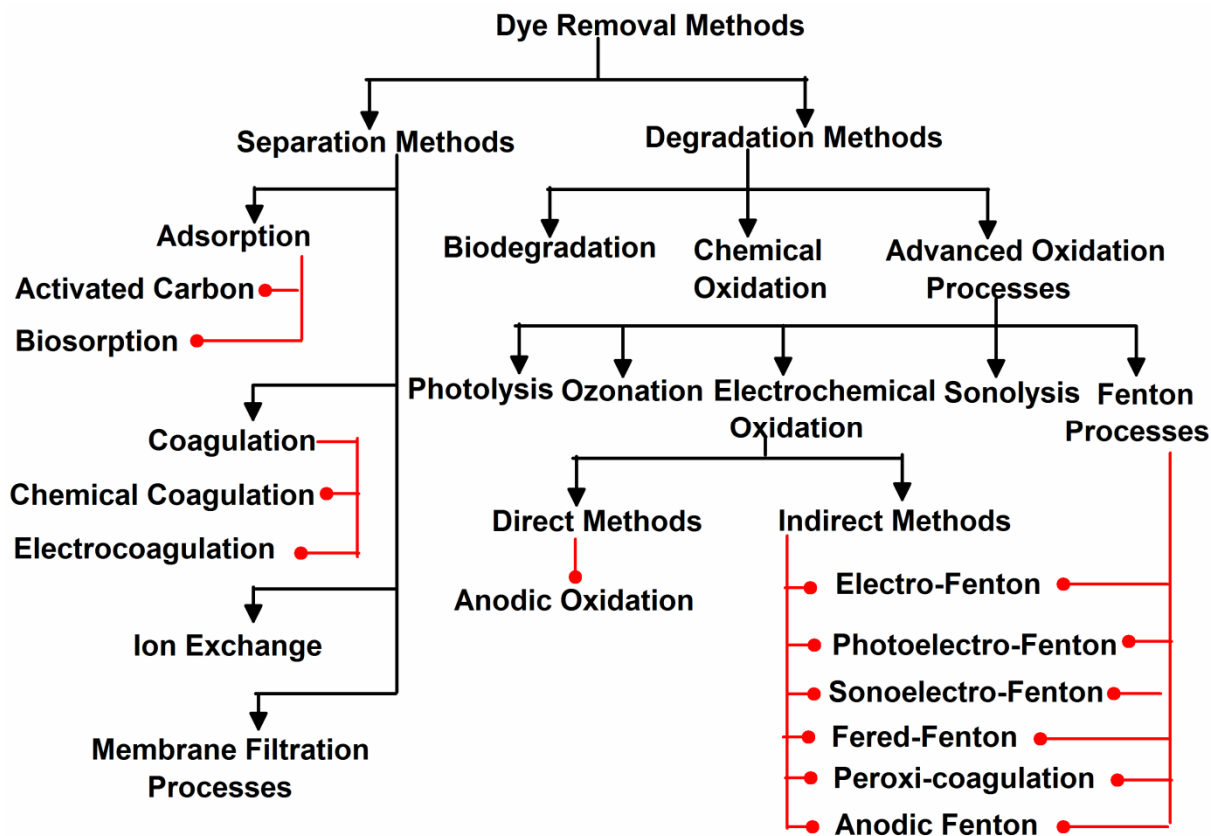
83

84

85 **2. Electrochemical advanced oxidation processes for dye removal**

86 Various treatment techniques such as adsorption, coagulation, filtration,
87 electrocoagulation, photolysis, sonolysis, biodegradation, wet land treatment, ozonation,
88 photocatalysis, membrane filtration etc. have been used for removing synthetic dyes from
89 aqueous solution. Advantages and disadvantages of dye removal methods have been
90 discussed in detail (Crini, 2006; Martinez-Huitle and Brillas, 2009; Nidheesh et al., 2013).
91 Based on the principle mechanism behind the removal of dyes, these processes can be
92 divided into two broad classes: Separative (physical, and physicochemical) methods, and
93 degradative (chemical and biological) methods. The schematic diagram of the various
94 methods used for the dye removal is shown in Fig. 1. Most of the methods used for dye
95 removal are separation process and the main disadvantage of these processes is the disposal
96 of dye containing sludge as in coagulation process, dye sorbed adsorbents and concentrated
97 dye solution as in membrane processes. In contrary to this, complex dye compounds undergo
98 a series of degradation in chemical degradation methods. In the case of use of advanced
99 oxidation processes, degradation procedure advance until ultimate oxidation degree, i.e.
100 mineralization of organic pollutants. These methods produce carbon dioxide, water and
101 various inorganic ions (following heteroatoms presents at the starting organic pollutants) as
102 the final products.

103



104

105

Fig. 1 Schematic representation of method used in dye removal from water

106

107

108

109

110

111

112

113

114

115

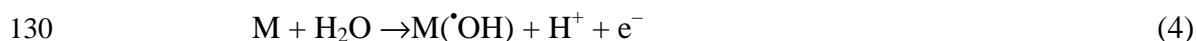
116

Among various degradation techniques, advanced oxidation processes (AOPs) received great attention for the efficient degradation of dyes, during recent years (Martinez-Huitle et al., 2009, Oturan and Aaron, 2014). These processes are based on the production of highly reactive oxidants, mainly hydroxyl radical ($\cdot\text{OH}$). This radical is the second most powerful oxidizing agent (after fluorine) with a redox potential of $E^\circ (\cdot\text{OH}/\text{H}_2\text{O}) = 2.8 \text{ V/SHE}$. Once these radicals are produced in situ, they attack organic pollutants with high reaction rates through following three different ways (Oturan, 2000; Brillas et al., 2009; Sirés et al., 2014): electron transfer (redox reaction) (Eq. (1)), H atom abstraction (dehydrogenation) (Eq. (2)), and electrophilic addition to π systems (hydroxylation) (Eq. (3)). These reactions produce organic radicals and start a radical chain including reactions with oxygen (formation of peroxy radicals) and formed reaction intermediates undergo further oxidation reactions with

117 generated oxidizing agents ($\cdot\text{OH}$, $\text{HO}_2\cdot$, $\text{H}_2\text{O}_2\dots$) until the complete mineralization of organic
118 pollutants.



122 Among the AOPs, electrochemical advanced oxidation processes (EAOPs) that have
123 been developed during the last decade have generated great interest for the abatement of
124 various persistent organic pollutants including synthetic dyes. EAOPs use electrolytically
125 produced hydroxyl radicals for the mineralization of organic pollutants. Based on the
126 production of hydroxyl radicals in the electrolytic system, EAOPs can be divided into two
127 categories: direct and indirect EAOPs as shown in Fig. 1. In the case of direct EAOPs,
128 hydroxyl radicals are produced on the anode surface by direct oxidation of water according to
129 the Eq. (4):



131 with M: anode material. The production rate and extent depend on the nature (catalytic
132 activity) of anode material, diffusion rate of organic pollutants on the active sites of anode
133 and applied current density (Panizza and Cerisola 2009; Miled et al., 2010). The great
134 advantage of this process is to not require the external addition of reagents for the production
135 of hydroxyl radicals. In the case of indirect EAOPs, the generation of hydroxyl radicals is
136 based on the Fenton chemistry including *in situ* electrochemical generation (electro-Fenton)
137 or externally addition of the one of the reagent (H_2O_2 or ferrous iron) (ferred-Fenton). Mostly
138 H_2O_2 is *in situ* produced at the cathode thanks to the use of an adequate electrode material.
139 Hydroxyl radicals are produced by the reaction between electrolytically generated or
140 externally added H_2O_2 and anodically generated or externally added ferrous iron (Brillas et

141 [al., 2009](#)). Electro Fenton process constitutes an excellent example of indirect EAOPs, in
142 which hydroxyl radicals are produced by the reaction between electrochemically *in situ*
143 generated H₂O₂ and electrocatalytically regenerated ferrous ion.

144 EAOPs have several advantages over conventional treatment techniques. The main
145 advantage of the EAOPs is environmental compatibility as the main reagent for all the
146 EAOPs is electron, which is an inbuilt clean species ([Peralta-Hernández et al., 2009](#)). Other
147 advantages are related to their versatile nature, higher pollutant removal efficiency,
148 operational safety and amenability of automation ([Jüttner et al., 2000](#); [Anglada et al., 2009](#),
149 [Sirés et al., 2014](#)). In addition, the presence of salt (e.g., NaCl) in wastewater could help to
150 improve process efficiency and reduce energy consumption ([Zhou et al., 2011a, 2011b](#)).

151 The main aim of this review is to present a general review on the application of EAOPs
152 for the removal of dyes from aqueous solution. Special attention is made on fundamental
153 reactions involved of each EAOP to provide clear idea on its characteristics and oxidation
154 capacity.

155

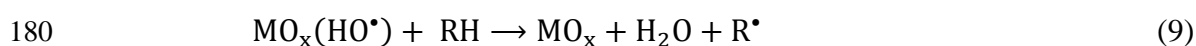
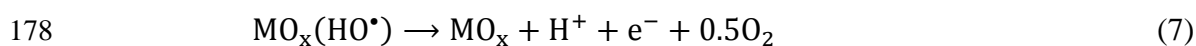
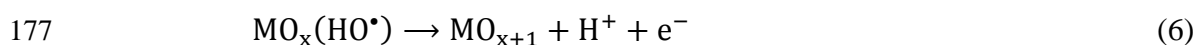
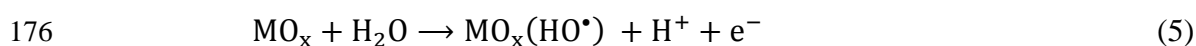
156 **3. Direct EAOPs**

157 Direct EAOPs produces hydroxyl radicals in the electrochemical reactor without the
158 external addition of chemicals. Anodic oxidation (called also electrooxidation) is the best
159 example of direct EAOPs. The following section explains the recent trends in dye removal by
160 anodic oxidation process.

161 **3.1 Anodic Oxidation**

162 Anodic oxidation (AO) is the most popular direct EAOPs; it works based on the
163 hydroxyl radical production at the anode surface ([Panizza and Cerisola, 2009](#)). The process is
164 heterogeneous and hydroxyl radicals formed are adsorbed on the anode surface. They are

165 chemisorbed in the case of active anode like Pt or DSA and are less available. The production
 166 of hydroxyl radicals is promoted by high O₂ evolution overvoltage anodes such as boron-
 167 doped diamond (BDD) thin film anodes. In these latter cases, hydroxyl radicals are
 168 physisorbed and consequently more available for oxidation of organics. Various researchers
 169 well explained the organic pollutant degradation mechanism in AO process in the case of
 170 metal oxide (MO_x) anodes (Comninellis, 1994; Scialdone, 2009). Heterogeneous hydroxyl
 171 radicals MO_x(HO•) are mainly formed by the oxidation of water (Eq. (5)). The adsorbed
 172 radicals result in the production of chemisorbed oxygen (Eq. (6)) or oxygen evolution (Eq.
 173 (7)). The chemisorbed oxygen also undergoes further reaction and produces oxygen as in Eq.
 174 (8). The MO_x(HO•) and oxygen oxidize the organic pollutant as in Eqs. (9) and (10). The
 175 surface of the anode is catalytically regenerated according to Eqs. (7)-(10).



182 There are two ways of pollutant degradation mechanism in AO process (Comninellis
 183 and Battisti, 1996): electrochemical conversion: degradation of persistent organic pollutants
 184 into biodegradable byproducts such as short-chain carboxylic acids, and electrochemical
 185 combustion or incineration (complete mineralization of organic pollutants into CO₂, H₂O and
 186 inorganic ions). Between the oxidants produced in AO electrolytic cell, MO_x(HO•) causes the
 187 complete mineralization of the organic pollutants and the chemisorbed oxygen
 188 (MO_x(HO•)) causes the selective oxidation of organic pollutants (Chen, 2004). This

189 difference in the oxidation ability of these two oxidants is mainly due to their different
190 oxidation potentials. Overall, AO process can be defined as the direct EAOPs in which the
191 degradation of the organic pollutants occurs mainly by the adsorbed hydroxyl radicals
192 produced by the water oxidation in the presence of high O₂ overvoltage anodes.

193 Compared with other treatment processes, AO process has several advantages. The
194 major three advantages of AO process are (Chen et al., 2003): rapid degradation of pollutants,
195 elevated removal efficiency, and easy operation. Apart from this, high efficiency at various
196 solution pH is also promotes the practical implementation of AO process. In general hydroxyl
197 radical formation is better in acidic media but the difference is not significant. Thus it was
198 reported that heterogeneous hydroxyl radicals are also formed at pH ≥ 10 (Sirés et al., 2006;
199 Özcan et al., 2008a). Even though complete mineralization of clofibric acid (Sirés et al.,
200 2006) and 4,6-dinitro-o-cresol (Flox et al., 2005) at pH 12 was reported.

201 In AO, selection of anode affects significantly the efficiency of the process. There are
202 two types of anodes in AO process: active and non-active anodes. This differentiation is
203 mainly based on the reaction of anode material with adsorbed hydroxyl radicals. In the case
204 of active anodes, formation of higher oxides or super oxides occurs by the reaction of anode
205 with hydroxyl radicals. This reaction happens when the anode has higher oxidation potential
206 above the standard potential required for the oxygen evolution (Migliorini et al., 2011). The
207 anodes like Pt, IrO₂, SnO₂ and RuO₂ are the examples of active anodes. On the other hand,
208 hydroxyl radicals are physically sorbed on the non-active anodes and the mineralization of
209 organic pollutants occurs mainly by the direct reaction of physisorbed hydroxyl radicals.
210 These electrodes do not contribute any direct anodic reaction of organic pollutants and do not
211 impart any catalytic site for the effective pollutant sorption (Migliorini et al., 2011). BDD
212 electrode is the best example of non-active anodes.

213 Compared to active electrodes, non-active electrodes have high mineralization capacity.
214 For example, BDD anode was found to be the best electrode for the mineralization of various
215 persistent organic pollutants. This is mainly due to its greater O₂ overvoltage (which
216 increases the hydroxyl radical production rate), its wide potential window, low background
217 current and very low activity for O₂ evolution reaction (Braga et al., 2010; Migliorini et al.,
218 2011; Oturan et al., 2012; Haidar et al., 2013). The removal of adsorbed organics on the BDD
219 surface is also easy. In most of the cases, rinsing with appropriate solvent is required for the
220 effective cleaning of BDD surface (Migliorini et al., 2011). The degradation of carboxylic
221 acids by Pt is also very difficult. But the degradation of these acids is feasible with BDD
222 anode, thanks to the efficiency of BDD([•]OH) and also the strong oxidants such as
223 peroxodisulfate and O₃ formed during oxidation process according to the following reactions
224 (Muruganathan et al., 2007; Flox et al., 2009; Li et al., 2010a).



228 Recently a great attention has been paid to improve the efficiency of anodes by using
229 appropriate substrate (Wang et al., 2013; Hu et al., 2014). The selection of suitable substrate
230 is also an important parameter. A substrate should have good electrical conductivity,
231 sufficient mechanical strength, and electrochemical inertness or easy formation of protective
232 films on substrate surfaces by passivation (Chen et al., 2003). For example, various substrates
233 like Si, Ti, Nb etc. were used as substrate for BDD anode. The substrate used for the BDD
234 anode has been classically Si. But, Si is difficult to use as a substrate for electrode due to its
235 fragile nature and its conductivity is strongly dependent on the experimental environments
236 (Sun et al., 2011). Among the various substrates, the suitable substrate for the BDD anode

237 was found as Ti (Chen et al., 2003; Sun et al., 2011). Also, the O₂ overvoltage potential of
238 Ti/BDD is higher than that of Si/BDD anode (Chen, 2004).

239 Dye removal from aqueous solution using the AO process has been studied by various
240 researchers. Faouzi et al. (2007) reported a total degradation and mineralization of alizarin
241 red S by AO process using BDD anode. Similarly, complete mineralization of methyl orange
242 in the presence of *in situ* microwave activated Pt was observed by Zhao et al. (2009). Color
243 and COD removals from real textile effluents using BDD anode was studied by Martínez-
244 Huitle et al. (2012) and they observed an effective reduction in color and COD after 15 h of
245 electrolysis. Yavuz and Shahbazi (2012) used bipolar trickle tower reactor containing BDD
246 anode for the removal of reactive black 5 in a continuous flow mode operation and achieved
247 97% color, ~51% COD and 29.3% TOC removal at the optimal conditions, along with the
248 reduction in toxicity. The oxidation of methyl orange using BDD anode in a 3 L capacity
249 electrolytic cell was studied by Ramírez et al. (2013) and obtained a 94% decolorization and
250 63.3% TOC removal efficiencies at the optimal conditions. Complete color and COD
251 removals from an aqueous solution containing methylene blue in the presence of BDD anode
252 was observed by Panizza et al. (2007). Degradation of three azoic dyes, Congo red, methyl
253 orange, and eriochrome black T, using conductive-diamond anodes was investigated by
254 Canizares et al. (2006) and concluded that the efficiency of the system depends only on the
255 initial concentration of dye.

256 Nava et al. (2008) compared the color and COD removal efficiencies of various
257 electrode materials for the abatement of alphazurine A dye and observed almost complete
258 mineralization of dye with Pb/PbO₂ and Si/BDD electrodes, while Ti/IrO₂ disfavored such
259 process. Similarly complete removal of color and COD induced by the alphazurine A using
260 BDD anode was observed by Bensalah et al. (2009). Aquino et al. (2013) used Si/BDD anode
261 for the degradation of reactive red 141 in a filter-press flow cell and applied response surface

262 methodology to determine the effects of different operating parameters on color, COD and
263 TOC removals. The performances of Ti–Pt/ β -PbO₂ and BDD anodes on the removal of
264 reactive orange 16 in a filter press reactor were investigated by [Andrade et al. \(2009\)](#). The
265 study concluded that even though complete dye removal is achieved by both the electrodes,
266 BDD provided better results than Ti–Pt/ β -PbO₂ due to less energy consumption. [Abdessamad
267 et al. \(2013\)](#) compared the efficiency of monopolar and bipolar BDD electrodes for the
268 removal of alizarin blue black B and concluded that the dye degradation efficiency of bipolar
269 AO system is 1.2 times higher than that of monopolar AO system. [Chen et al. \(2003\)](#) were
270 found that dye removal efficiency of Ti/BDD anode was higher than that of Ti/Sb₂O₅–SnO₂
271 anode. Also, Ti/BDD anode has higher dye removal efficiency in the cases of alizarin red S
272 ([Sun et al., 2011](#)), orange II and reactive red HE-3B ([Chen et al., 2003](#)). The dye removal
273 efficiencies of BDD and PbO₂ electrodes were compared by [Panizza and Cerisola \(2008\)](#) and
274 observed a higher oxidation rate and higher current efficiency in the case of BDD anode than
275 that of PbO₂ anode. At the same time, methyl orange degradation efficiency of TiRuSnO₂ is
276 very much less than that of BDD and PbO₂ anode ([Labiadh et al., 2016](#)). Partial removal of
277 the dye was achieved by using TiRuSnO₂ anode, but complete dye removal was also
278 observed with other anodes. Even though, both anodes are efficient for the complete dye
279 removal, complete mineralization was occurred only in the presence of BDD anode.

280 [Yao et al. \(2013\)](#) prepared PbO₂-ZrO₂ nanocomposite electrodes by pulse
281 electrodeposition and used it for the removal of methylene blue. The authors observed a
282 100% dye and 72.7% COD removal after 120 min of electrolysis. Similarly, [An et al. \(2012\)](#)
283 synthesized TiO₂-NTs/Sb–SnO₂/PbO₂ anode for the abatement of C.I. reactive blue 194 and
284 reported that the prepared electrode has a high decolorization and mineralization ability.
285 Recent study by [do Vale-Júnior et al. \(2016\)](#) demonstrates that Sn-Cu-Sb alloy anode
286 prepared by cold gas spray is very efficient for the degradation of dyes from water medium.

287 The authors observed complete acid blue-29 removal and mineralization after 300 min and
288 600 min of electrolysis, respectively.

289 Effect of boron doping in BDD anode on dye removal was investigated by [Migliorini et al. \(2011\)](#)
290 and reported that highly boron doped electrodes has the higher reactive orange 16
291 removal efficiency. Similar result has been observed by [Bogdanowicz et al. \(2013\)](#).

292 [Rodriguez et al. \(2009\)](#) observed two different oxidation mechanisms for acid yellow 1
293 in the presence of BDD anodes. The oxidation of dye depends more on its initial
294 concentration. At the lower dye concentration, the oxidation process followed pseudo first
295 order kinetics and under the control of mass transport. While, at the higher dye
296 concentrations, the degradation of acid yellow 1 followed zero order kinetics and reaction
297 kinetics was controlled by charge transfer.

298 [Panizza and Cerisola \(2008\)](#) observed the pH independent methyl red oxidation in the
299 range of 3 to 7. Similarly, insignificant effect of initial solution pH on dye removal by AO
300 process using Ti/SnO₂-Sb/PbO₂ was observed by [Song et al. \(2010\)](#). Similar result has been
301 reported by [Petrucci and Montanaro \(2011\)](#). The authors observed that even though the color
302 removal was affected by the change in pH, the mineralization ability of BDD anode was not
303 altered with the solution pH.

304 Supporting electrolyte also plays an important role on the dye removal mechanism.
305 [Aquino et al. \(2012\)](#) studied the effects of the salt (supporting electrolyte) addition for the
306 removal of acid blue 62, reactive red 141, direct black 22, and disperse orange 29 using
307 conductive-diamond anodes. The authors observed a mediated electrooxidation of dyes in the
308 presence of chloride addition. At the same time, the removal of dyes by the addition of
309 sulphate as supporting electrolyte is mainly by the attack of hydroxyl radicals, generated from
310 BDD anode. [Zhou et al. \(2011a\)](#) compared the methyl orange degradation by electrochemical

311 oxidation using BDD and mixed metal oxide anodes and found enhanced dye removal in the
312 presence of NaCl, which is mainly attributed to the co-action of mediated oxidation from
313 active chlorine species.

314 The functional groups presents in the dyes also affects the efficiency of the electrolytic
315 system. [Saez et al. \(2007\)](#) compared the alizarin red and eriochrome black T removals in the
316 presence of BDD anode. The authors reported two different oxidation mechanisms for dye
317 removals, even though complete COD and color removals from both dye wastewaters were
318 observed. The removal of alizarin red was mainly due to hydroxyl radical mediated oxidation
319 and controlled by mass transfer process, while the removal of eriochrome black T was mainly
320 due to electrolytically generated reagents like peroxodisulphate.

321

322 **4. Indirect EAOPs**

323 Production of hydroxyl radicals in indirect EAOPs is accomplished by the in situ
324 production or external addition of chemicals. Fenton based EAOPs are the best examples of
325 indirect EAOPs. The following sections discuss the applications and recent advances in these
326 processes for the removal of dyes from aqueous medium.

327 **4.1 Electro-Fenton (EF) process**

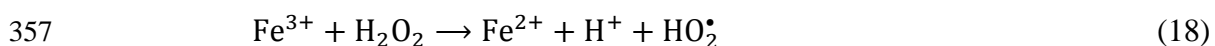
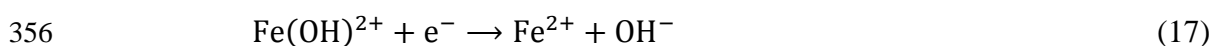
328 During the last decade EF process received much attraction among other processes.
329 This is an economically and environmentally friendly process to remove efficiently toxic
330 and/or persistent organic pollutants from water. Oturan and Brillas groups reported the
331 principles of the EF process in the starting of 2000 ([Oturan and Pinson 1995](#); [Brillas et al., 1996](#);
332 [Oturan, 2000](#); [Brillas et al., 2000](#)). EF process is an attractive tool and its interest is
333 mainly due to its high degrading effectiveness of persistent organic pollutants, fast pollutant

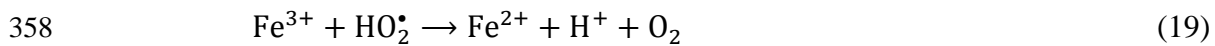
334 removal rate and environmental compatibility (Oturán et al., 2000; Brillas et al., 2009;
335 Nidheesh et al., 2013; Sirés et al., 2014; Vasudevan and Oturan 2014).

336 EF process works based on the *in situ* electrogeneration of Fenton's reagent, a mixture
337 of H₂O₂ and Fe²⁺ which is the origin of the Fenton's reaction (Eq. (15)) to generate hydroxyl
338 radicals. Hydrogen peroxide is generated continuously at the cathode surface from the two
339 electron reduction of O₂ in the acidic medium (Eq. (14)) (Oturán et al., 2008a; Özcan et al.,
340 2009a; Nidheesh and Gandhimathi, 2012). Supply of oxygen near the cathode during EF
341 treatment is required for fulfilling the continuous production of hydrogen peroxide in the
342 electrolytic system. The addition of a catalytic amount of a ferrous salt (to produce Fe²⁺ ions)
343 into the solution leads to production of •OH according to Fenton's reaction (Eq. (15)).



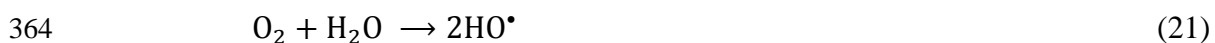
346 Catalysis of the Fenton's reaction by electrochemical regeneration of ferrous ion is an
347 important advantage of EF process compared to conventional Fenton process (Oturán et al.,
348 2011; Moreira et al., 2013). Indeed, the optimal pH value for Fenton's reaction and Fenton
349 related processes is about 3 (Brillas et al., 2009). At this pH, the predominant species of iron
350 is Fe(OH)²⁺ (Eq. 16) (Özcan et al., 2013). The Fe³⁺ produced by Fenton's reaction remains
351 under the form of Fe(OH)²⁺ and undergoes cathodic reduction to produce ferrous ion
352 according to Eq. (17) (Özcan et al., 2008b). Apart from this main source, ferrous ions are
353 regenerated in the EF process via Fenton's chain reactions as in Eqs. (18-20) (Oturán et al.,
354 2004; Oturan et al., 2010a).





360 where R[•] is organic radical.

361 Also, in overall, EF process results the production of two moles of hydroxyl radicals from 0.5
362 moles of oxygen as in Eq. (21) (Oturan et al., 2001) showing the catalytic behavior of the
363 process.



365 An insignificant change in solution pH with electrolysis time is the other advantage of
366 EF process. This is mainly due to the counterbalancing of proton consumed during the Fenton
367 reaction by the protons produced via water oxidation at the anode (El-Desoky et al., 2010)
368 and carboxylic acids generated during the oxidation process (Oturan and Aaron, 2014).

369 Carbonaceous materials are widely used as the cathode, which is the working electrode
370 of EF process. This is mainly due to its wide range of electrochemical activity for O₂
371 reduction and low catalytic activity for H₂O₂ decomposition (Panizza and Cerisola, 2001).
372 Also, the porosity of carbonaceous material is very high, in particular 3D carbon materials
373 like carbon felt or graphite felt are of high porosity. These pores are useful for the sorption of
374 oxygen gas supplied near the cathode surface and consequently results in higher amount of
375 hydrogen peroxide generation. Various carbonaceous materials like carbon-felt (Oturan,
376 2000; Murati et al., 2012), reticulated vitreous carbon sheet (El-Desoky et al., 2010; Ghoneim
377 et al., 2011), activated carbon fiber (Wang et al., 2010), graphite (George et al., 2013, 2016;
378 Nidheesh et al., 2014a), commercial graphite-felt (Khataee et al., 2009; Panizza and Oturan,
379 2011) and chemically or electrochemically modified graphite felt (Zhou et al., 2013; 2014),
380 carbon sponge (Özcan et al., 2008c) etc. were used as the cathode material for the efficient
381 electrogeneration of hydrogen peroxide in EF cell. Özcan et al. (2008c) compared the dye

382 degradation efficiency of carbon sponge and carbon-felt for the abatement of acidified basic
383 blue 3 solutions and found that carbon sponge is the effective cathode than carbon felt for EF
384 process. By analyzing the reported literatures, various forms of Pt have been used frequently
385 as anode in EF cell for the degradation of various organic pollutants (Nidheesh and
386 Gandhimathi, 2012; Sopaj et al., 2015, 2016).

387 The efficiency of EF process increases by combining AO and EF processes. This can be
388 achieved by the use of an O₂ overvoltage anode in the EF process along with the
389 carbonaceous cathode. Oturan et al. (2012) showed that this process was able to mineralize
390 quasi-completely the herbicide atrazine and its by-product cyanuric acid which already
391 reported many times to be recalcitrant to hydroxyl radicals.

392 EF process has been proved as an efficient tool for the abatement of dyes from water
393 medium. Nidheesh and Gandhimathi (2014a) used graphite-graphite electrolytic system for
394 the abatement of rhodamine B (RhB) at pH 3. The authors reported that with the increase in
395 electrode immersion depth the efficiency of the electrolytic system also increases. This is
396 mainly due to the increased contact between cathode surface and air bubbles and the authors
397 recommended to use bubble column reactor with lengthy electrode for the efficient removal
398 of organic pollutants. Similarly, complete destruction of azure B and 95% TOC abatement at
399 the end of 8 h EF treatment was observed by Olvera-Vargas et al. (2014). Almomani and
400 Baranova (2013) analyzed the dye removal efficiencies of single and two compartment cells
401 in the presence of stainless steel cathode and BDD anode and observed that two compartment
402 cell is better than single cell for the removal of dyes from aqueous medium. Lakhimi et al.
403 (2007) investigated the depollution of methylene blue, Congo red and yellow drimaren using
404 carbon felt cathode and Pt sheet anode and observed a rapid degradation of dyes in their
405 single and mixture solution. Almost complete mineralization of dyes also observed by
406 Guivarch et al. (2003) and Guivarch and Oturan (2004). Similarly, 95% of the initial TOC

407 caused by alizarin red (Panizza and Oturan, 2011) and acid red 97 (Kayan et al., 2010) was
408 removed effectively using the graphite-felt and carbon-felt cathodes, respectively. Diagne et
409 al. (2014) compared the efficiencies of AO and EF processes for the removal of indigo dye
410 and observed higher mineralization efficiency for EF process. Complete mineralization of the
411 dye was observed within 2 h of electrolysis. Yu et al. (2015) modified graphite felt by using
412 carbon black and PTFE; and observed 10.7 times higher H₂O₂ production compared to
413 unmodified electrode. EF process using this modified graphite felt cathode is efficient for
414 complete removal of 50 mg L⁻¹ methyl orange within 15 min and 95.7% TOC removal at 2 h
415 electrolysis; this efficiencies being more than 4 times that of EF process operated with raw
416 graphite felt cathode.

417 Apart from, solution pH, catalyst dosage, initial pollutant concentration, electrode area,
418 applied current and inner electrode spacing; the hardness in the water also affects the
419 efficiency of EF process significantly (dos Santos et al., 2016). The presence of magnesium
420 and calcium in water medium reduced the dye removal efficiency of EF process for the dye
421 eriochrome black T. This reduction in the performance of EF process is mainly related to the
422 difficulty to break the divalent cation- eriochrome black T complex by •OH.

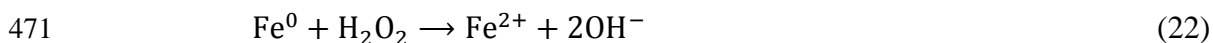
423 Xu et al. (2014) prepared graphene doped gas diffusion electrode using modified
424 Hummers' method and used for the removal of reactive brilliant blue in a three electrode
425 undivided cell of volume 200 mL. The study concluded that under the optimal conditions,
426 80% of the dye and 33% of TOC were removed after 180 min of electrolysis by the novel
427 electrode. Ghoneim et al. (2011) observed a complete dye removal and 97% of mineralization
428 by EF process in an electrolytic cell of 600 mL capacity containing reticulated vitreous
429 carbon cathode, platinum gauze anode and 0.2 mM sunset yellow FCF azo dye. Sirés et al.
430 (2008) compared the dye removal efficiency of EF cell with carbon-felt cathode for the
431 degradation of crystal violet (CV), fast green FCF (FCF), methyl green (MeG) and malachite

432 green (MG). In this study, it was observed that the absolute rate constant for their reaction
433 with hydroxyl radicals increases in the order MeG < FCF < CV < MG. Total depollution of a
434 dye mixture containing the above four dyes with a COD of 1000 mg L⁻¹ was also observed.
435 Complete decolorization and approximately 85–90% mineralization of levafix red CA and
436 levafix blue CA was observed by [El-Desoky et al. \(2010\)](#). Similar results were obtained in the
437 cases of real dyeing wastewater ([Wang et al., 2010](#)), reactive blue 4 ([Gözmen et al., 2009](#)),
438 direct orange 61 ([Hammami et al., 2007](#)), etc.

439 [Lin et al. \(2014\)](#) studied orange II removal behavior of EF process in a divided cell and
440 reported that dye removal rate in cathodic compartment was much faster than that in anodic
441 compartment. [Scialdone et al. \(2013\)](#) performed the abatement of acid orange 7 in a
442 microfluidic reactor and reported that the process is efficient for the usage of cheaper and
443 easier to handle graphite as cathodic material, mainly due to the sufficient oxygen production
444 from the anode. Therefore, external addition of air or oxygen is not required for this type of
445 reactor. [Iglesias et al. \(2013a\)](#) used airlift continuous reactor for the removal of reactive black
446 5 and lissamine green B and accomplished high decolorization percentages at high residence
447 times. Methyl orange removal in a 3 L capacity pilot flow plant was studied by [Isarain-
448 Chávez et al. \(2013\)](#) and obtained 80% of decolorization efficiency at the optimal conditions.
449 Nanostructured ZnO-TiO₂ thin films deposited on graphite felt anode ([El-Kacemi et al.,
450 2016](#)) exhibited higher dye removal and mineralization efficiency. Within 60 min of
451 electrolysis Amido black 10B dye was discolored and the mineralization efficiency of the EF
452 process reached 91% after 6 h of electrolysis. Application of graphene based electrode
453 material improves the efficiency of EF process in a noticeable manner ([Yang et al., 2017](#)).
454 Graphene ([Zhao et al., 2016](#)), graphene doped graphite-PTFE ([Xu et al., 2014](#)), reduced
455 graphene oxide coated carbon felt ([Le et al., 2015](#)), graphite felt modified with

456 electrochemically exfoliated graphene (Yang et al., 2017) electrodes exhibited excellent
457 hydrogen peroxide generation potential and subsequent dye removal efficiency.

458 Ferrous ion is the worldwide accepted Fenton catalyst for the generation of hydroxyl
459 radical (Oturán and Aaron, 2014). Apart from this, other forms iron like zero-valent iron
460 (Fe^0) and ferric ions (Fe^{3+}) can be used as Fenton catalyst. Addition of Fe^{3+} instead of Fe^{2+}
461 undergoes the ferrous ion regeneration reaction prior to Fenton reaction. Fe^0 addition leads to
462 the production of Fe^{2+} by the reaction between hydrogen peroxide as in Eq. (22) (Fu et al.
463 2010a). Oturan et al. (2008a) used ferric ion instead of ferrous ion for the degradation of
464 malachite green in Pt/CF cell at pH 3. The authors observed a total decolorization within 22
465 min and total mineralization within 540 min of electrolysis at an applied current of 200 mA.
466 Özcan et al. (2009b) investigated the acid orange 7 removal by EF process using ferric ions
467 and 92% of TOC removal was reported. Nidheesh and Gandhimathi (2014b) compared the
468 RhB) removal efficiencies of Fe^0 , Fe^{2+} and Fe^{3+} in graphite-graphite EF system. The rate of
469 dye removal at the optimal conditions follows the order of $\text{Fe}^0 > \text{Fe}^{3+} > \text{Fe}^{2+}$. But the optimum
470 amount of Fenton's reagent followed the order of $\text{Fe}^0 \sim \text{Fe}^{2+} > \text{Fe}^{3+}$.

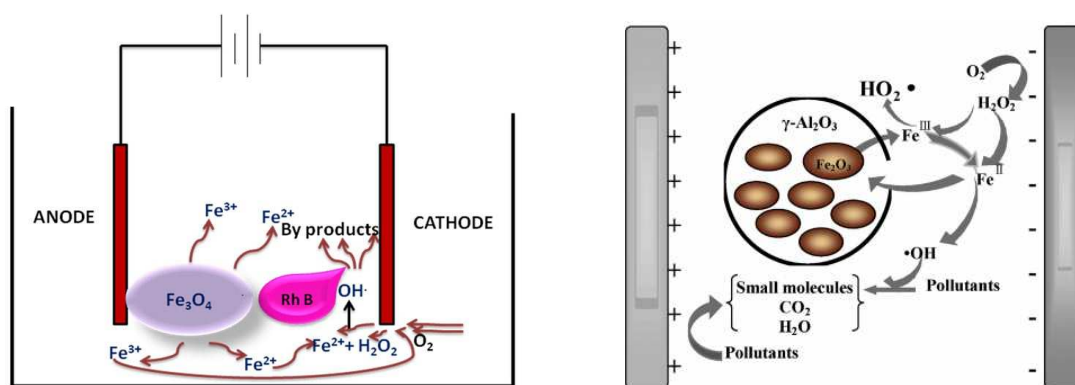


472 Persistent organic pollutant abatement using EF like process also received a great
473 attention in recent years. The transition metals having more than one oxidation states and
474 having a difference of unity in oxidation states can undergo Fenton like reactions as shown in
475 Eq. (23). Various transition metals like Mn (Balci et al., 2009; George et al., 2014; Nidheesh
476 and Gandhimathi, 2014b), Cu (Oturán et al., 2010b; George et al., 2013b; Nidheesh and
477 Gandhimathi, 2014b), Co (Oturán et al., 2010b), Ag (Oturán et al., 2010b), Ni (George et al.,
478 2014) etc. have been used as EF like catalyst for the abatement of various pollutants.



480 Recently, the EF related researches focused on the heterogeneous EF system (Nidheesh,
481 2015). In this process, solid catalysts containing iron species are used as the iron source
482 instead of ferrous salts. Heterogeneous catalyst can be reused several times for the
483 degradation of organic pollutants. Recently Oturan and co-workers proposed EF-pyrite
484 process and found it to be very efficient for the mineralization of various organic pollutants
485 (Amar et al., 2015; Barhoumi et al., 2015; 2016). Labiadh et al. (2015) used this technology
486 for the removal of 4-amino-3-hydroxy-2-p-tolylazo-naphthalene-1-sulfonic acid, an azo dye
487 from water medium and found complete mineralization of 175 mg L⁻¹ dye within 8 h of
488 electrolysis. Nidheesh et al. (2014a) prepared magnetite by the chemical precipitation method
489 and used for the decolorization of RhB. The authors used magnetite containing various
490 concentrations of ferrous and ferric ions and found that the magnetite with Fe(II)/Fe(III) ratio
491 2:1 and 1:2 has good dye removal efficiency than other catalysts. At the optimal conditions,
492 97% of RhB was removed effectively by the heterogeneous EF process. Similarly EF
493 oxidation of acid red 3R in the presence of Fe₂O₃/γ-Al₂O₃ was investigated by Yue et al.
494 (2014) and it was reported 77% dye removal within 100 min of electrolysis. Rosales et al.
495 (2012) used Fe alginate gel beads for the removal of azure B and lissamine green B; and
496 obtained almost complete removal of dyes from aqueous solution. Iglesias et al. (2013a) used
497 the same catalyst for the decolorization of reactive black and lissamine green B 5 in an airlift
498 continuous reactor. Iron loaded sepiolite was used as a heterogeneous EF catalyst for the
499 removal of reactive black 5 in a continuous flow mode of operation (Iglesias et al., 2013b)
500 and obtained 80 to 100% dye removal at the optimal conditions. Liang et al. (2016)
501 investigated the effect of five metals (Cu, Ce, Mn, Fe and Co) and their loading contents on
502 methyl orange degradation, observing the highest activity on Co/GDE and good stability
503 toward wide pH ranges (3–9).

504 The dye removal mechanism of heterogeneous EF process is illustrated in Fig. 2. Iron
 505 species from the heterogeneous catalyst are released into the solution and reacts with the
 506 hydrogen peroxide produced at the cathode surface as in conventional Fenton process. In
 507 some of the cases, the Fenton reactions may occurs at the solid catalyst surface, without the
 508 dissolution of iron species. At these conditions the catalyst should be in suspension or
 509 efficient mixing should be there for the effective removal of organic pollutants.

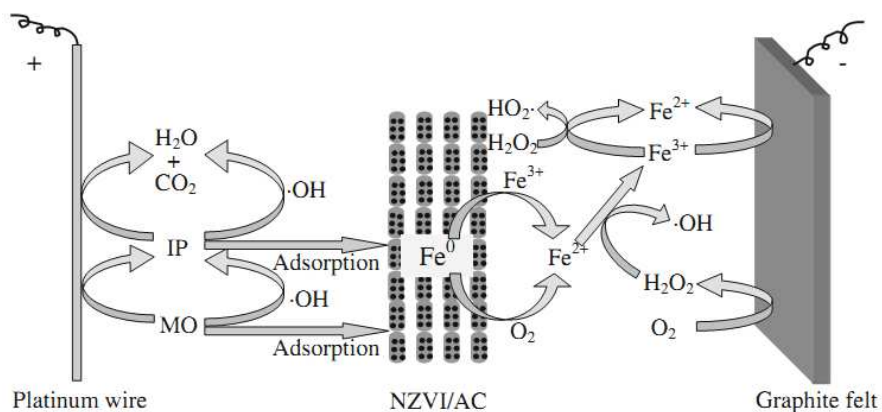


510 **Fig. 2** Dye removal mechanism of heterogeneous EF process using (a) magnetite (Nidheesh
 511 et al., 2014d), (b) $\text{Fe}_2\text{O}_3/\gamma\text{-Al}_2\text{O}_3$ (Yue et al., 2014). Reprinted with permission from *RSC Adv.*,
 512 Copyright 2014 RSC and *J. Ind. Eng. Chem.*, Copyright The Korean Society of Industrial and
 513 Engineering Chemistry and Elsevier 2013, respectively.

514 Another trend in EF process is the application of three dimensional (3D) electrolytic
 515 cells for the abatement of persistent organic pollutants. 3D EF process is similar to the
 516 conventional two electrode system. But it contains particle electrode as the third electrode.
 517 Particle electrode is generally a granular material, which may contain iron oxides and filled
 518 between anode and cathode. Iron loaded inert substances and iron oxides can be used as the
 519 particle electrode for the EF system. Polarization of the particle electrode occurs during the
 520 electrolysis. Due to the polarization, these particles converts as a large numbers of charged
 521 microelectrodes with anode in one surface and cathode in other surface (Zhang et al., 2013).

522 These electrodes reduce the pollutant concentration by the sorption process, increasing the
 523 ionic strength of the electrolytic cell and supplying additional iron species in the system. In
 524 EF process, the particle electrodes predominately act as a heterogeneous EF catalyst (Wang et
 525 al., 2014a). Thus the efficiency of 3D EF system is higher than conventional EF system due
 526 to its large electrode surface and higher mass transfer (Wang et al., 2008a). The COD
 527 removal efficiency of 3D system should be 10-15% higher than that of conventional EF
 528 system (Zhang et al., 2013).

529 Zhang et al. (2014) used nanoscale zero-valent iron/activated carbon (NZVI/AC) as a
 530 heterogeneous Fenton catalyst in 3D EF system for the removal of methyl orange (MO). 20-
 531 30% of methyl orange mineralization efficiency increment was observed with the addition of
 532 the heterogeneous Fenton catalyst. More than 80% of dye removal efficiency after 10 min of
 533 electrolysis and 40% of TOC after 2 h of electrolysis were observed. Based on the
 534 experimental results, the authors proposed the degradation mechanism of MO in 3D EF
 535 system as in Fig. 3.



536
 537 **Fig. 3** Methyl orange degradation mechanism in a 3D EF system (where, MO is methyl
 538 orange, NZVI/AC is nanoscale zero-valent iron/activated carbon and IP is intermediate
 539 products). Reprinted from Zhang et al. (2014), Copyright 2014, Springer-Verlag Berlin
 540 Heidelberg.

541 Wang et al. (2014b) used catalytic particle electrodes derived from steel slag and
542 manganese loaded on the particle electrodes by ultrasound impregnation calcinations
543 approach for the removal of RhB from aqueous solution by 3D EF process containing Pt
544 anode and stainless steel cathode. The authors observed a complete removal of dye within 50
545 min of electrolysis. Electrolysis of real dyeing wastewater in the presence of graphite raschig
546 rings particle electrode, Pt/Ti plate anode and graphite cathode was carried out by Wang et al.
547 (2008a). The authors attained a 70.6% color removal under specific operation conditions in
548 150 min. Wang et al. (2014a) used particle electrode prepared from steel slag for the removal
549 of RhB and obtained 82.4% and 65.45% of RhB removal with and without of air supply
550 within 60 min of electrolysis.

551 Removal of dyes from water medium using EF process under continuous flow mode
552 was tested by Nidheesh and Gandhimathi (2015a, b). The authors used bubble column reactor
553 (BCR) of capacity 3L for the removal of RhB from aqueous solution. They studied the effects
554 of applied voltage, solution pH, catalyst concentration and inlet flow rate on the removal of
555 dyes in continuous flow mode. At the optimal conditions, 98% of the RhB solution having an
556 initial concentration of 50 mg L⁻¹ was removed effectively using the BCR under continuous
557 flow mode. Similarly, EF process operated in BCR is highly efficient for the treatment of real
558 textile wastewater (Nidheesh and Gandhimathi, 2015b). Due to the increased mass and
559 electron transfer, flow-through EF reactor (in which solution is flow through anode and
560 cathode) was found more energy-efficient and more pollutant removal efficiency than
561 conventional EF reactor (Ma et al., 2016; Ren et al., 2016).

562 Even EF or related processes are very efficient for the abatement of various persistent
563 organic pollutants from water medium; the incomplete mineralization of these pollutants may
564 cause further environmental pollution. Some of the intermediate compounds are more toxic
565 than their parent compounds. For example, Le et al. (2016) carried out the toxicity analysis

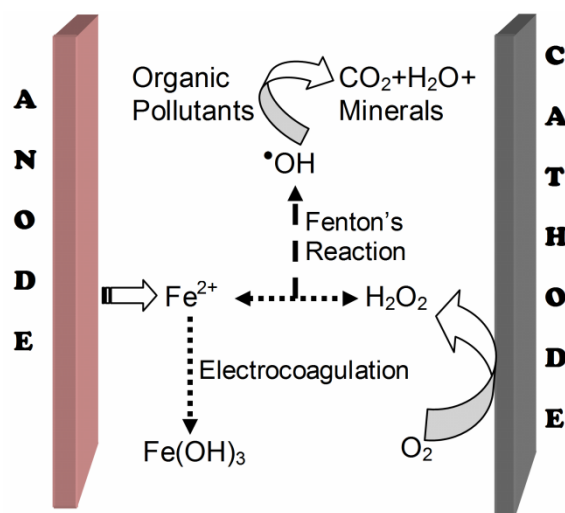
566 during the acid orange 7 degradation via EF process. In the initial periods of electrolysis, the
567 toxicity values increased abruptly and are very much higher than that of acid orange 7. This is
568 mainly due to the generation of more toxic intermediate products such as 1,2-naphthaquinone
569 and 1,4-benzoquinone. The subsequent degradation of these compounds resulted in the
570 production of carboxylic acids and decreased the toxicity values significantly. But,
571 phytotoxicity and microbial toxicity of real textile wastewater has been reduced significantly
572 after 1 h EF treatment (Roshini et al., 2017).

573

574 **4.2 Peroxi-coagulation**

575 Peroxi-coagulation is a modified EF process which use iron or stainless steel as anode
576 for supplying ferrous ions in water medium, instead of external ferrous ion addition as in EF
577 process. Ferrous ions continuously generated from anode by oxidation of a sacrificial anode
578 according to Eq. (24). In the case of use an appropriate cathode able to generate H₂O₂ and O₂
579 supply, Fenton's reaction takes place to form [•]OH. With the increase in electrolysis time,
580 ferric ions accumulates in the aqueous medium leads to the formation of Fe(OH)₃ precipitate.
581 Thus, peroxi-coagulation process is a combination of EF and electrocoagulation, in which
582 organic pollutants are removed by the attack of hydroxyl radicals (degradation process) and
583 coagulation with iron precipitates (Brillas and Casado, 2002). This process was firstly applied
584 for the removal of aniline from aqueous medium (Brillas et al., 1997). The overall reactions
585 occurring in a peroxi-coagulation cell along with organic pollutants removal mechanism are
586 shown in Fig. 4.





588

589

Fig. 4 Working principles of peroxi-coagulation process

590

591

592

593

594

595

596

597

598

599

600

601

602

Increase in solution pH with electrolysis time is the difference in peroxi-coagulation with EF process (Venu et al., 2014, 2016). Hydrogen evolution reaction by the water reduction at the cathode surface (Eq. (25)) is the main reason behind the raise in solution pH (Drogui et al., 2008). This increase in pH increases also the rate $\text{Fe}(\text{OH})_3$ formation and causes electrocoagulative removal of pollutants along with oxidative action Fenton's reaction. This results in a higher amount of sludge production in the electrolytic cell. Brillas and Casado (2002) observed higher pollutant removal efficiency for peroxi-coagulation than EF process for currents ≥ 10 A and this is mainly attributed to the effective removal of intermediate compounds formed (by the attack of hydroxyl radicals) and by coagulation (adsorption or imprisonment in $\text{Fe}(\text{OH})_3$). The sludge formation in the peroxi-coagulation cell can be reduced by maintaining the solution pH to 3. At these conditions, the iron (III) concentration in the system is less than that of ferrous or ferric ions, results in Fenton's reaction to take place more efficiently.

603



604

605

A few studies have been reported for the dye removal by peroxi-coagulation process. Zarei et al. (2010a) used peroxi-coagulation process for the removal of four dyes namely C.I.

606 basic red 46, C.I. basic blue 3, C.I. basic yellow 2 and malachite green from aqueous solution
607 at pH 3 and reported about 90% of dye removal within 10 min electrolysis. [Salari et al.](#)
608 [\(2009\)](#) reported that peroxi-coagulation process has the ability to decolorize 90% of the dye
609 in less than 30 min and 81% mineralization of dye at 6 h. Similar results were reported by
610 [Zarei et al. \(2009\)](#).

611 Sludge formation in peroxi-coagulation process can be reduced by regulating the
612 solution pH to 3. [Nidheesh and Gandhimathi \(2014 d\)](#) reported that pH regulated peroxi-
613 coagulation has higher dye removal efficiency than that of pH unregulated peroxi-coagulation
614 process. But the authors observed scavenging effects by the addition of sodium salts
615 containing chloride, bicarbonate, carbonate and sulphate. For maintaining the pH, the authors
616 used sulphuric acid and regulated the solution pH to 3 at every 15 min interval. This
617 increased the concentration of sulphate ions in the cell. By the addition of sodium salts,
618 higher amount of sulphate salts precipitate produces (as per common ion effect according to
619 Le Chatelier's principle) and form a layer at the cathode surface. The authors observed a
620 white layer formation on the cathode surface after the electrolysis, and this layer contains
621 higher amount of sodium sulphates. This layer was removed with the insertion of cathode in
622 an acid solution. Due to this layer formation, the volume of active pores at cathode surface
623 reduces and results in lesser hydrogen peroxide formation. This causes a reduction in dye
624 removal efficiency by the addition of sodium salts.

625 [Nidheesh and Gandhimathi \(2014c\)](#) compared the decolorization and degradation
626 efficiencies of EF, peroxi-coagulation (PC) and pH-regulated peroxi-coagulation (PC-pH)
627 processes from real textile wastewater. Based on the experimental results, the authors
628 concluded that the color and COD removal efficiency of EF process is mainly by the
629 oxidation of pollutants and the efficiency of peroxi-coagulation is mainly by the combination
630 of oxidation and separation processes. The authors observed a higher sludge production for

631 PC and PC-pH processes at higher pH values and concluded that the higher removal
632 efficiencies at higher pH values is mainly by electrocoagulation process. The sludge
633 produced from PC process was reused as a heterogeneous EF catalyst for the abatement of
634 same real textile wastewater and observed 97% of color, 47% of COD and 33.2% TOC
635 reductions.

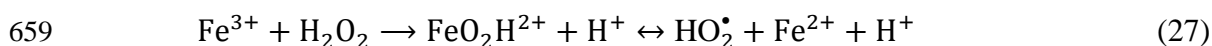
636

637 **4.3 Fered-Fenton and Anodic Fenton processes**

638 Fered-Fenton process is a modified form of Fenton process, in which hydrogen
639 peroxide and ferrous ions are added externally to the electrolytic cell and then ferrous iron
640 regenerated electrochemically from reduction of Fe^{3+} formed in Fenton's reaction (Eq. 15) for
641 the improvement of process efficiency (Brillas et al., 2009). This process is also known as
642 EF-Fere and is suitable for the abatement of organic pollutants with high TOC value and
643 lower biodegradability. With the addition of hydrogen peroxide and ferrous iron salt,
644 conventional Fenton's reaction occurs between ferrous ion and hydrogen peroxide and $\cdot\text{OH}$
645 produced following Fenton's reaction (Eq. 15) results in the reduction of organic loading.
646 Further reduction of organic pollutant can be attributed to conventional Fenton process
647 assisted by electrochemistry since Fenton's reaction is catalyzed by the regeneration of
648 ferrous ions from the electrochemical reduction of ferric ions (Brillas et al., 2009).

649 Anodic Fenton process is a Fenton related electrochemical peroxidation process. It can
650 be considered as a modified form of peroxi-coagulation process. One of the major
651 disadvantages of peroxi-coagulation process is the sludge production due to the formation of
652 $\text{Fe}(\text{OH})_3$ in excess of iron(III) in the solution. The main problem for this is the lack of
653 sufficient quantity of hydrogen peroxide production at the cathode surface (As per
654 conventional Fenton's reaction, the theoretical ratio of ferrous to hydrogen peroxide is 1. But

655 in peroxi-coagulation process, the concentration of ferrous ion increases and that of hydrogen
656 peroxide comes to saturation or decreases with electrolysis time). This results in higher
657 sludge formation and may cause scavenging reactions as given below (Brillas et al., 2009).



660 This can be reduced by the external addition of hydrogen peroxide, known as anodic Fenton
661 process. Ghosh et al. (2012) studied the degradation of methylene blue and titan yellow dye
662 solutions using this method (but authors mentioned it wrongly as EF process) and observed
663 98% and 96% respective dyes removal after 60 min of electrolysis at pH 3, 1 mM of H₂O₂
664 and current density of 4.31 mA cm⁻². Eslami et al. (2013) compared the efficiencies of anodic
665 Fenton process (but authors mentioned it wrongly as EF process) with conventional Fenton
666 process for the removal of color and COD from real textile wastewater and higher removal
667 efficiency for anodic Fenton process was observed. The decolorization and COD removal
668 efficiencies of anodic Fenton process after 60 min of electrolysis were found as 72.9% and
669 70.6%, respectively, within 350 mA current and externally added 1978 mg L⁻¹ H₂O₂
670 concentration. At the same time, 52.3% of color and 51.2% of COD were removed via
671 Fenton process after 120 min of treatment at 1978 mg L⁻¹ H₂O₂ concentration and 250 mg L⁻¹
672 of ferrous ion concentration.

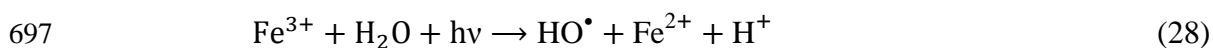
673 In order to improve the efficiency of anodic Fenton process and to reduce the negative
674 effect of hydroxyl ions produced by the water reduction at cathode, Saltmiras and Lemley
675 (2000) used divided electrolytic cell. Anode cell and cathode cell are connected with a salt
676 bridge. Then the anode cell is enriched with the electrolytically generated ferrous ions and
677 Fenton reactions occur with the external addition of hydrogen peroxide. Thus, anodic Fenton
678 process reduces the external addition of large quantity of iron salts as in conventional Fenton

679 process and the effluent pH can be partially neutralized by combining the treated solutions
680 from each cells (Wang and Lemley, 2002). But the scale up of anodic Fenton with a salt
681 bridge is a little difficult task because the salt bridge requires frequent replacement of the
682 saturated NaCl solution (Wang and Lemley, 2003). To overcome this, Lemley group
683 developed membrane anodic Fenton process, in which an ion exchange membrane used
684 between anode cell and cathode cell, instead of salt bridge.

685

686 4.4 Photoelectro-Fenton process

687 A combination of UV radiation along with EF process, known as photoelectro-Fenton
688 (PEF) process, produces more hydroxyl radicals than that in conventional EF process. This
689 enhances the rate of dye degradation by the Fenton's reaction. The additional hydroxyl
690 radicals are produced by the photochemical reduction of Fe³⁺ ions from UV light irradiation
691 as in Eq. 28 (Brillas et al., 1998 a, b; Muruganandham and Swaminathan, 2004). On the other
692 hand the regeneration of Fe²⁺ ions by this reaction (Eq. (28)) catalyzes also the Fenton's
693 reaction (Eq. 15) to produce more [•]OH. The photolysis of *in situ* produced H₂O₂ in the
694 presence of UV light also produces additional [•]OH according to Eq. (29) (Brillas, 2014), but
695 the amount of [•]OH produced by this reaction is not significant because of very low absorption
696 coefficient of H₂O₂.



699 Production of hydroxyl radicals and regeneration of ferrous ions from the photodegradation
700 of iron complexes and ferric carboxylates is another advantage of PEF over conventional EF
701 process. The photo-reduction of ferric hydroxyl complexes especially Fe(OH)²⁺ produces
702 additional [•]OH as in Eq. 30 (Gogate and Pandit, 2004; Kavitha and Palanivelu, 2004; Brillas

703 [2014](#)). Similarly, photo-reactive ferric carboxylates also undergoes degradation process and
704 produces additional ferrous ions and $\cdot\text{OH}$ according to [Eq. \(31\)](#) ([Brillas, 2014](#)).

705 Many researchers put an interest on dye removal using PEF process. [Khataee et al.](#)
706 [\(2014\)](#) compared the efficiency of EF and PEF processes for the abatement of C.I. Acid Blue
707 5 under recirculation mode with a cathode containing multi walled carbon nanotubes. The
708 authors observed dye removals of 98% after 60 min of electrolysis for PEF processes.
709 Similarly, [Bedolla-Guzman et al. \(2016\)](#) compared the efficiencies of anodic oxidation, EF
710 and PEF processes for the degradation of Reactive Yellow 160 dye, using BDD anode. The
711 authors observed dye removal efficiency order as: PEF>EF>anodic oxidation. Similar results
712 are reported by [Solano et al. \(2015\)](#) for the degradation of Congo red dye and [El-Ghenymy et](#)
713 [al. \(2015\)](#) for the abatement of malachite green oxalate dye. [Khataee et al. \(2010a\)](#) used
714 carbon nanotube-polytetrafluoroethylene cathode for the removal of C.I. basic red 46 by the
715 oxalate catalyzed PEF process and compared its efficiency with the efficiencies of EF and
716 PEF processes. The authors reported that oxalate catalyzed PEF process has higher dye
717 removal efficiency than that of PEF and EF process. Abatement of 244 mg L^{-1} Acid Red 29
718 by PEF process using BDD anode and carbon-PTFE cathode in an undivided cell was studied
719 by [Almeida et al. \(2012\)](#) and observed an almost complete dye mineralization. [Garcia-Segura](#)
720 [et al. \(2012\)](#) compared the Direct Yellow 4 degradation efficiencies of EF, PEF and photo-
721 assisted EF process. Photo-assisted EF was performed by applying EF treatment for a
722 particular time, followed by the photolysis of treated dye solution. They reported higher dye
723 removal efficiency for PEF process (almost total mineralization). The authors also observed
724 an equivalent dye removal capacity of PEF process for photo-assisted EF process after giving
725 sufficient time for the EF process to produce intermediates that can be mineralized by the
726 photolysis. [Peralta-Hernández et al. \(2008\)](#) compared the Orange II removal efficiencies of
727 direct photolysis, EF and PEF processes and observed 31%, 63% and 83% of TOC removals,

728 respectively. Mineralization of Acid Red 14 by PEF process using an activated carbon fiber
729 cathode was examined by Wang et al. (2008b) and compared its efficiency with EF process.
730 The authors observed 60–70% mineralization efficiency for EF process and more than 94%
731 mineralization efficiency for PEF process. Mineralization and decolorization of aqueous
732 solution containing Acid Violet 7 and Reactive Black 5 by EF and PEF processes using a
733 vitreous carbon electrode cathode was studied by Salazar and Ureta-Zañartu (2012) and
734 observed more than 90% mineralization efficiency for PEF process.

735 The pseudo first order rate of dye removal by PEF process was modeled as a function
736 of catalyst concentration, initial dye concentration, solution pH, applied current and flow rate
737 by Khataee et al. (2014). The authors reported the rate constant as:

$$738 \quad k_{\text{app}} = 1310.4 \frac{[\text{CA}]^{0.48} I^{0.55}}{[\text{Dye}]^{1.07} \text{pH}^{1.75} Q^{0.84}} \quad (32)$$

739 where, k_{app} is the apparent rate constant following first order kinetic, CA is the catalyst
740 concentration in mM, I is the applied current in A, Q is the flow rate in L h⁻¹.

741 Coupling of conventional photocatalysis with PEF process received great attention in
742 recent years. The principles of photocatalysis were explained well by various researchers
743 (Bahemann, 2004; Girish Kumar and Gomathi Devi, 2011; Rauf et al., 2011; Lam et al.,
744 2012). Iranifam et al. (2011) used ZnO nanoparticles as the photo catalyst for the removal of
745 C.I. Basic Yellow 28 from aqueous solution and compared the dye removal efficiencies of
746 ultraviolet-C (UV-C), EF, UV/ZnO, PEF and PEF/ZnO processes. The authors found the
747 decreasing color removal efficiency order as: PEF/ZnO > PEF > UV/ZnO > EF > UV-C.
748 Similarly, Khataee and Zarei (2011) reported the C.I. Direct Yellow 12 removal efficiency
749 order as: PEF/ZnO > PEF > EF > UV/ZnO. Photocatalytic treatment of C.I. Acid Red 17 using
750 immobilized TiO₂ nanoparticles combined with PEF process was investigated by Khataee et
751 al. (2010b) and it was observed the color removal decreasing order as: PEF/UV/TiO₂ > PEF >

752 EF > UV/TiO₂. The authors observed 93.7%, 85.9%, 66.8% and 20% decolorization
753 efficiencies for PEF/UV/TiO₂, PEF, EF and UV/TiO₂ processes respectively. Similar order
754 was reported by [Zarei et al. \(2010b\)](#) for the removal of C.I. Basic Red 46. The authors
755 observed 98.8% mineralization of 20 mg L⁻¹ C.I. Basic Red 46 dye at 6 h of electrolysis using
756 PEF/TiO₂ process.

757

758 **4.5 Solar Photoelectro-Fenton**

759 PEF process has been found as an effective tool for the abatement of dyes from water
760 medium. But the higher energy consumption of artificial UV light used in PEF process
761 increases the operational cost of this process ([Brillas, 2014](#)). In order to solve this
762 disadvantage of PEF process and to increase the chance of applying this process in the real
763 field, [Brillas' group \(Flox et al., 2007a, 2007b\)](#) proposed a modified form of PEF process,
764 known as solar photoelectro-Fenton (SPEF) process for the degradation and removal of
765 various organic persistent pollutants. In this process, the EF treated wastewater is irradiated
766 with sunlight ($\lambda > 300$ nm), instead of artificial UV light as in PEF process. Therefore, SPEF
767 method is cheap, uses renewable energy source, high energy efficient, amenable to
768 automation, versatile and safe ([Martínez-Huitle and Brillas, 2009](#); [Brillas, 2014](#)). It is also
769 found that the efficiency of SPEF is higher than that of PEF process due to the greater
770 intensity of UVA and UVB lights of sunlight which can photolyze the ferric carboxylate
771 complexes more rapidly ([Garcia-Segura et al., 2013](#); [Brillas, 2014](#)). Also, compared to EF
772 process, SPEF process is more potent than EF, with higher mineralization efficiency, higher
773 current efficiency and lower energy consumption ([Salazar et al., 2011](#)). [Garcia-Segura and](#)
774 [Brillas \(2016\)](#) compared the performance of SPEF for the degradation of monoazo, diazo and
775 triazo dyes in water medium. Acid Orange 7, Acid Red 151 and Disperse Blue 71 were
776 considered as the model monoazo, diazo and triazo dyes, respectively. SPEF process is very

777 much efficient for the degradation of monoazo dye with almost complete mineralization after
778 3 h of electrolysis. At the same time, the dye degradation efficiency of SPEF is high for triazo
779 dye than diazo dye.

780 [Ruiz et al. \(2011a\)](#) used 2.5 L flow plant for the degradation of Acid Red and Acid
781 Yellow from water medium. The electrolytic cell was equipped with carbon-PTFE cathode
782 and BDD anode. The solar photo-reactor having irradiated volume of 600 mL and containing
783 mirror at bottom with a horizontal inclination of 30⁰. The authors observed a rapid
784 decolorization of both dyes by the EF process, but the mineralization rate was low. This low
785 mineralization rate of EF process is mainly due to the higher concentration of persistent
786 carboxylic acids and their iron-complexes. But the photolysis of this electrolyzed solution
787 leads to almost total mineralization of dye wastewater. [Ruiz et al. \(2011b\)](#) used same reactor
788 for the removal of Acid Yellow 36 from aqueous solution and observed the similar results as
789 explained above. Degradation of Disperse Red 1 and Disperse Yellow 3 using SPEF process
790 was examined by [Salazar et al. \(2011\)](#) and observed total mineralization of both dyes.

791

792 **4.6 Sonoelectro-Fenton:**

793 Application of ultrasound for the treatment of water and wastewater received a great
794 attention during the recent years ([Gogate et al., 2002](#); [Sivasankar and Moholkar, 2010](#); [Bagal
795 and Gogate, 2014](#)). Acoustic cavitation is the forcing phenomenal for the degradation of
796 organic pollutants in the presence of ultrasound in water medium. It is the process of
797 formation, growth, and succeeding collapse of microbubbles or cavities due to ultrasound in a
798 water medium ([Gogate and Pandit, 2004](#)). The collapse of bubbles occurs within 50 ns, and
799 the process is almost adiabatic ([Chakma and Moholkar, 2013](#)), results in the generation of
800 higher pressure (in the range of 500–5,000 bar) and temperature (in the range of 1,000–

801 15,000 K) in the reactor (Suslick, 1989). Due to this cavitation phenomenon, hydroxyl
802 radicals are formed as given below (Li et al., 2010).



804 where U refers to the application of ultrasound.

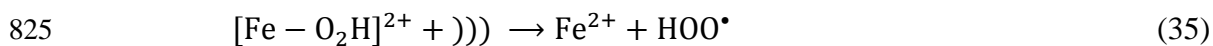
805 Addition of ultrasound in EF process, known as sonoelectro-Fenton (SEF) process
806 (Oturán et al., 2008b), results in a higher amount of radicals in the water medium and thus
807 higher removal efficiency than EF process. In the presence of ultrasound, the electrolytically
808 produced hydrogen peroxide dissociated into hydroxyl radicals as:



810 Oturán et al. (2008b) reported the order of relevance of the enhancing factors in SEF
811 process as: (1) enhanced production of hydroxyl radical and Fenton reaction kinetics by the
812 improved mass transfer rate of both reactants (ferric ions and oxygen) towards the cathode
813 surface for the electrochemical generation of Fenton's reagent and its transfer into the
814 solution, (2) the additional hydroxyl radical generation by the sonolysis, and (3) pyrolysis of
815 organics at the time of bubble explosion.

816 Li et al. (2010) observed an increased hydrogen peroxide production with the addition
817 of ultrasound in EF cell. The hydrogen peroxide produced in SEF process is higher than the
818 sum of hydrogen peroxide concentration produced from EF and sono Fenton processes. This
819 improvement can be related to enhancement of mass transfer by sonolysis Oturán et al.
820 (2008b).

821 In the presence of ultrasound, the regeneration of ferrous ions from intermediate
822 complex produced via conventional Fenton process also occurs as in Eq. (35) (Pradhan and
823 Gogate, 2010; Bagal and Gogate, 2014). This results in an enhancement of Fenton reactions
824 in the electrolytic cell.



826 The arrangement of sono probe (one type of ultrasound source) and electrode also affects the
827 efficiency of SEF process. There are three types of probe-electrode arrangement ([Compton et](#)
828 [al., 1997](#)) in a sono-electrochemical reactor, namely face-on, side-on and sonotrode. Among
829 this arrangement, face-on orientation has higher mass transfer capability and is depends on
830 ultrasound power, electrode-horn distance and electrode area ([Ramachandran and Saraswathi,](#)
831 [2011](#)). These authors also tested the efficiency of angular geometry and compared with that
832 of face-on orientation. But the mass flux values of face-on orientation are two to three times
833 higher than that of angular geometry. Thus, face-on geometry is the better probe-electrode
834 arrangement in a SEF reactor. This arrangement reduces the layer formation on the cathode
835 surface and enhances the efficiency of SEF process. Thus the enhancement in the efficiency
836 of SEF process is mainly due to physical and chemical mechanisms ([Babuponnusami and](#)
837 [Muthukumar, 2012](#)). Physical mechanism related to the high mixing and electrode surface
838 cleaning by the addition of ultrasound in the EF reactor. This enhances the mass transfer
839 between electrode and solution in addition to higher hydrogen peroxide production. The
840 chemical mechanism is due to the additional radical formation in the cell as explained above.

841 SEF process has been found as an efficient tool for the abatement of dyes from aqueous
842 solution. An enhancement in hydrogen peroxide production and dye removal rate with the
843 addition of ultrasound in EF process was observed by [Li et al. \(2010b\)](#). Authors concluded
844 that in SEF process, low frequency ultrasound has a positive effect on dye mineralization.
845 The rate of dye removal by SEF process is 10 fold higher than that of sonolysis and 2 fold
846 higher than that of conventional Fenton process ([Martínez and Uribe, 2012](#)). Abatement of
847 reactive blue 19 dye using SEF process was investigated by [Siddique et al. \(2011\)](#). The
848 authors observed an almost complete removal of dye and 56.47% of TOC from un-
849 hydrolyzed reactive blue 19 dye solution at a frequency of 80 kHz. At the same time, 81% of

850 TOC removal was observed for hydrolyzed reactive blue 19 solution. Similar way, 85% of
851 TOC and more than 90% of color introduced by azure B were removed efficiently by SEF
852 process in the presence of reticulated vitreous carbon cathode and platinum gauze counter
853 electrode (Martínez and Uribe, 2012). Oturan et al. (2008b) observed a synergistic effect in
854 SEF process (compared to EF process) in degradation of azobenzene at low frequencies (i.e.
855 20 and 60 80 kHz) and an improvement in degradation kinetics for early treatment times.
856 Similarly, Şahinkaya (2013) observed a negligible increase in treatment efficiency of SEF
857 process, when compared with the capital and operating costs of sonication. Lounis et al.
858 (2016) examined the performance of SEF for the degradation of Orange G in various water
859 mediums like pure water, natural water and seawater. The dye removal rate was very high in
860 sea water medium followed by pure water and natural mineral water. Complete dye removal
861 was observed for sea water and pure water medium, while 94% of dye removal was observed
862 for natural mineral water medium.

863

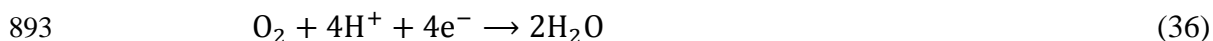
864 **4.7 Bioelectro Fenton**

865 Two versions of bioelectro-Fenton were reported: (i) bioelectro-Fenton (BEF) based on
866 bio-electrochemical reactor proposed by Zhu and Ni (2009) consisting of two cells: microbial
867 fuel cell (MFC) containing biodegradable organic substrates and anodic Fenton treatment
868 (AFT) cell containing pollutants to be degraded by EF process, and (ii) BEF consisting of
869 coupling between EF process and microbial degradation (Olvera-Vargas et al., 2016a, b). EF
870 step being utilized as pre-treatment for mineralization of beta-blocker drug metoprolol: 1 h
871 EF pre-treatment step followed by aerobic biodegradation allowed 90% mineralization at 4
872 days. On the other hand, Ganzenko et al., (2017) investigated the use of BEF during
873 treatment of a pharmaceutical wastewater treatment in two scenarios: EF as both pre-

874 treatment and post-treatment of biological step and found and found first scenario more
875 efficient.

876 [Feng et al. \(2010b\)](#) used BEF system containing anaerobic anode chamber having
877 *Shewanella decolorationis* S12 as microorganism for the generation of electricity and carbon
878 nanotube (CNT)/ γ -FeOOH composite cathode for the production of hydrogen peroxide. The
879 authors used this system for the abatement of orange II and observed a complete
880 decolorization and mineralization of dye. A maximum power output of 230 mW m^{-2} was also
881 obtained from the BEF system. But modification of BEF system with
882 polypyrrole/anthraquinone-2,6-disulfonate (PPy/AQDS) conductive film boosted the
883 performance of the system. [Feng et al. \(2010a\)](#) observed a maximum power density of 823
884 mW m^{-2} by the use this conductive film.

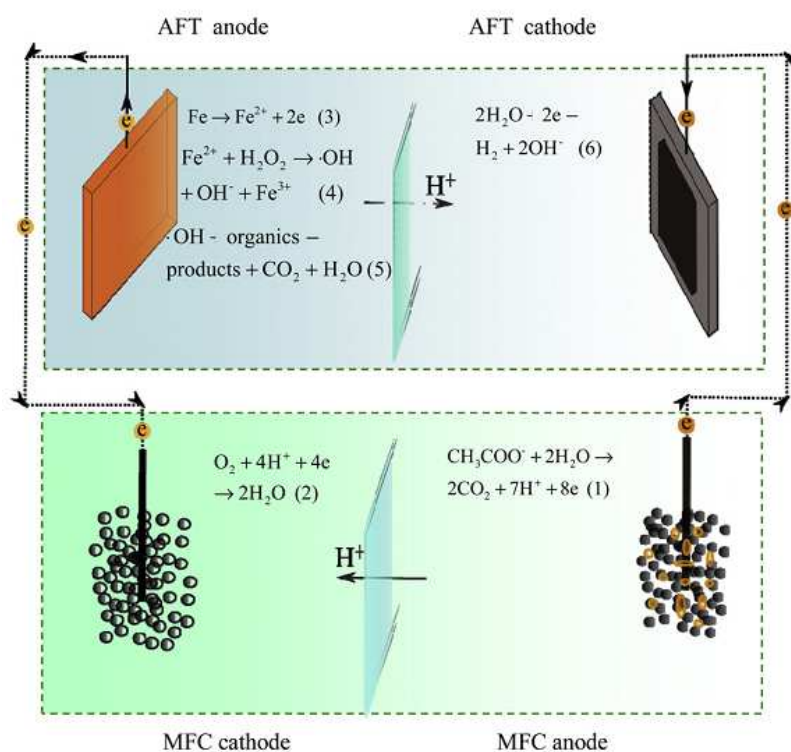
885 MFC is a “renewable energy device that converts energy available in organic
886 compounds to electricity via the canalization of microorganisms” ([Feng et al., 2010a](#)). The
887 biodegradable organic substance generally used in an MFC is glucose or acetate.
888 Microorganisms present on the anode compartment oxidize these substrates and generates
889 protons and electrons ([Zhu and Logan, 2013](#)). The electrons produced via this oxidation
890 process flow through an external circuit to cathode. At the same time, the protons released
891 into the solution. At the cathode surface, oxygen reacts with both proton and electron, forms
892 water as in [Eq. \(36\)](#).



894 Besides the electricity generation, MFC have several other advantages. Self-regeneration
895 capacity of microorganism reduces the catalyst cost in MFC compared to conventional
896 chemical fuel cells ([Fernándezde Dios et al., 2013](#)). Absence of pollutant generation

897 (including all toxic substances) during any operations in MFC makes this cell as an
 898 environmentally friendly energy system (Gong et al., 2011).

899 Rabaey and Rozendal, (2010) showed that a MFC can generate a voltage of 0.8 V to an
 900 open circuit and this low-voltage electricity can be used for other electrolytic process like
 901 hydrogen peroxide production in EF process. By this reaction, 78.85 mg L⁻¹ of H₂O₂
 902 production in the cell after 12 h of electrolysis was observed by Fu et al. (2010b). This
 903 hydrogen peroxide undergoes conventional Fenton's reaction and produces [•]OH. But in BEF,
 904 the production of hydrogen peroxide requires only two-electron transfer. Thus a BEF system
 905 generates electricity, produces [•]OH in cathodic compartment and causes degradation of
 906 organic pollutants. The working principles of a BEF system are shown in Fig. 5.



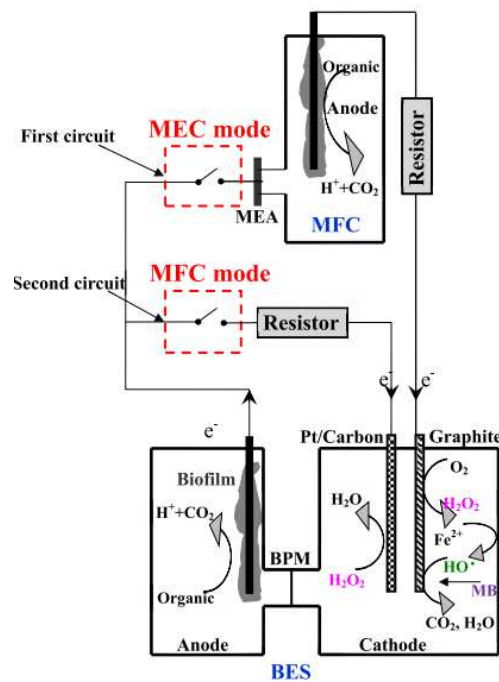
907
 908 **Fig. 5** Energy generation and subsequent pollutant removal reactions in MFC assisted-AFT
 909 system. Reprinted with permission from Liu et al., (2012). Copyright 2012, Elsevier.

910 Effect of MFC combined with *in situ* and *ex situ* EF processes on the abatement of dye
911 was examined by [Fernández de Dios et al. \(2013\)](#). The authors carried out the experiments
912 both in batch and continuous flow mode for the removal of lissamine green B and crystal
913 violet from aqueous solution. 94% of lissamine green B and 83% of crystal violet removals
914 were observed by the researchers after 9 h of electrolysis in MFC combined with *in situ* EF
915 process. For this condition, respective TOC amounts of 82% and 70% were removed from the
916 same BEF reactor respectively for lissamine green and crystal violet. At the same time more
917 than 95% of dye removal and 85% of TOC removal were observed in a bubble column
918 reactor used in MFC combined with *ex situ* EF process.

919 Recently, [Zhang et al. \(2015\)](#) developed a new BEF reactor capable of supplying
920 hydrogen peroxide and eliminating its residual concentration ([Fig. 6](#)). The investigators
921 achieved this by alternating switching between microbial electrolysis cell (MEC) and
922 microbial fuel cell (MFC). In MEC mode of operation, degradation of pollutants occurs by
923 the electrolytic generation of H₂O₂ and subsequent generation of hydroxyl radicals by the
924 reaction with ferrous ions. The residual hydrogen peroxide after the MEC mode of operation
925 consumes during the MFC mode of operation, by using hydrogen peroxide as electron
926 acceptor. The authors tested the efficiency of this BEF system for the abatement of 50 mg L⁻¹
927 methylene blue solution. Almost complete decolorization and mineralization of the dye
928 solution were achieved after 8 h and 16 h in MEC mode of operation. The residual hydrogen
929 peroxide concentration was observed as 180 mg L⁻¹ and this was consumed completely in
930 MFC mode of operation within 39 h of operation.

931 Coupling EF and microbial oxidation process is effective for treating real textile
932 wastewater ([Roshini et al., 2017](#)). Combined EF and aerobic-microaerophilic process is able
933 to remove 86.4% COD, 85.8% color and 56.1% TOC of textile wastewater. Similarly, 82.5%

934 COD, 52.7% color and 41% TOC were removed by EF process followed by aerobic
935 microbial process..



936

937 **Fig. 6** BEF reactor with alternate switching, where MEC: microbial electrolysis cell; MFC:

938 microbial fuel cell; MEA: membrane electrode assembly; BES: bioelectrochemical system;

939 BPM: bipolar membrane. Reprinted with permission from Zhang et al. (2015). Copyright

940

2015, Elsevier

941 5. Scale up of EAOPs cells

942 Application of EAOPs for the abatement of dyes was largely investigated at lab scale.

943 A few studies were investigated even in continuous flow mode of operation, which resembles

944 the practical conditions for the dye wastewater treatment. The next step of investigation is

945 pilot scale studies for dye removal by EAOPs. The scale up of an electrolytic reactor depends

946 on its geometric, kinematic, current/potential and thermal similarity between the reactors

947 (Gupta and Oloman, 2006). Geometric similarity can be achieved by keeping the dimensional

948 ratios as constant. But it is not advisable to increase the inner electrode spacing. Because,

949 with increase in electrode spacing, the ohmic drop between electrodes increases, which

950 results in reduction in the efficiency of EAOPs. The increased spacing requires higher
951 voltages for the optimal operation and this increases the energy consumption of the cell,
952 consequently increases the cost of operation. Therefore, during scale up process of
953 electrolytic reactors, geometric similarity is usually sacrificed in favor of current/potential
954 similarity (Gupta and Oloman, 2006). Current/potential similarity is also known as electrical
955 similarity; which can be achievable by keeping constant differences in electrode potential and
956 current density (Goodridge and Scott, 1994). This can be achieved by keeping a constant
957 inner electrode gap during scale up process. The kinematic similarity depends on the inlet
958 flow rate and this similarity can be achievable by keeping same residence time or flow rate
959 during the scale up process. Thermal similarity is another important parameter to be
960 considered during the scale up process. Most of the lab scale works were carried out at the
961 room temperature. But the effluents from the textile industry have the temperature near to the
962 100 °C. Therefore, a mismatching between the lab scale efficiency and real field efficiency
963 will occurs. Because in the case of Fenton based EAOPs, the elevated temperature decreases
964 the stability of oxygen and hydrogen peroxide. This decreases the efficiency of EAOPs at
965 elevated temperature.

966

967 **6. Conclusions and perspectives**

968 EAOPs have a great potential to remove dyes from water medium. Comparing to direct
969 EAOPs, indirect EAOPs, especially that based on Fenton chemistry has received increased
970 attention in the last decade. AO process, a well-known direct EAOPs, is also very efficient to
971 remove dyes from aqueous solution. The higher cost of high oxygen over potential anode is
972 one of the main drawbacks of this process. Various types of Fenton process based EAOPs,
973 naming EF, PEF, SEF, peroxi-coagulation, fered Fenton, anodic Fenton etc. have been
974 applied effectively for the removal of dyes. Total decolorization of dyes has been achieved in

975 most of the cases. But the mineralization efficiency is, in general, less than that of
976 decolorization efficiency. This is mainly due to the less degradation rate of by-products in all
977 the EAOPs. Ferrous ion is found as an efficient catalyst among various forms of iron for the
978 removal of dyes in EF and related processes. EF like reactions, heterogeneous EF and 3D EF
979 processes are the new trends in dye removal by EF based processes. The external addition of
980 iron salt has been replaced with sacrificial iron anode in peroxi-coagulation process. But the
981 sludge production and increased passivation rate of electrodes decreases the degradation
982 efficiency of this process. The efficiency of EF process has been increased significantly by
983 the addition of UV light (PEF) and ultrasound (SEF). The rate of removal of PEF and SEF
984 processes are generally higher than that of EF process, but these latest processes are more
985 costly because of coupling with highly energy consuming processes. The practical
986 implementation of PEF process has been simplified by the introduction of solar energy
987 (SPEF). Combined biological process and EAOPs is also a new trend in this field. In BEF,
988 electricity produced from MFC has been used for the production of hydroxyl radicals. But the
989 time taken for the removal of dyes by BEF is much higher than that of EF process.

990 Scale up of EAOPs is a global problem, even though these processes are very efficient
991 and cheap. Electrical similarity is the major factor to be remembered during scale up
992 operations. Since, this is very important for the real implementation of EAOPs, more works
993 on dye removal by EAOPs in industrial scale is required. Overall, it can be concluded that
994 EAOPs constitute a promising technology for the removal of dyes from aqueous solution.

995

996 **References**

- 997 Abdessamad, N., Akrouf, H., Hamdaoui, G., Elghniji, K., Ksibi, M., Bousselmi, L., 2013.
998 Evaluation of the efficiency of monopolar and bipolar BDD electrodes for electrochemical
999 oxidation of anthraquinone textile synthetic effluent for reuse. *Chemosphere* 93, 1309–
1000 1316.
- 1001 Abo-Farha, S.A., 2010. Comparative study of oxidation of some azo dyes by different
1002 advanced oxidation processes: Fenton, Fenton-like, photo-Fenton, and photo-Fenton-like.
1003 *J. Am. Sci.* 6 (10), 128–142.
- 1004 Almeida, L.C., Garcia-Segura, S., Arias, C., Bocchi, N., Brillas, E., 2012. Electrochemical
1005 mineralization of the azo dye acid red 29 (Chromotrope 2R) by photoelectro-Fenton
1006 process. *Chemosphere* 89 (6), 751–758.
- 1007 Almomani, F., Baranova, E.A., 2013. Kinetic study of electro-Fenton oxidation of azo dyes
1008 on boron-doped diamond electrode. *Environ. Technol.* 34 (11), 1473–1479.
- 1009 Ammar, S., Oturan, M.A., Labiadh, L., Guersalli, A., Abdelhedi, R., Oturan, N., Brillas, E.,
1010 2015. Degradation of tyrosol by a novel electro- Fenton process using pyrite as
1011 heterogeneous source of iron catalyst. *Water Res.* 74, 77–87.
- 1012 An, H., Cui, H., Zhang, W., Zhai, J., Qian, Y., Xie, X., Li, Q., 2012. Fabrication and
1013 electrochemical treatment application of a microstructured TiO₂-NTs/Sb–SnO₂/PbO₂
1014 anode in the degradation of C.I. reactive blue 194 (RB 194). *Chem. Eng. J.* 209, 86–93.
- 1015 Andrade, L.S., Tasso, T.T., da Silva, D.L., Rocha-Filho, R.C., Bocchi, N., Biaggio, S.R.,
1016 2009. On the performances of lead dioxide and boron-doped diamond electrodes in the
1017 anodic oxidation of simulated wastewater containing the reactive orange 16 dye.
1018 *Electrochim. Acta* 54 (7), 2024–2030.
- 1019 Anglada, A., Urtiaga, A., Ortiz, I., 2009, Contributions of electrochemical oxidation to waste-
1020 water treatment: fundamentals and review of applications. *J. Chem. Technol. Biotechnol.*
1021 84 (12), 1747–1755.
- 1022 Aquino, J.M., Rocha-Filho, R.C., Rodrigo, M.A., Sáez, C., Cañizares, P., 2013.
1023 Electrochemical degradation of the reactive red 141 dye using a boron-doped diamond
1024 anode. *Water Air Soil Pollut.* 224, 1397.
- 1025 Aquino, J.M., Rodrigo, M.A., Rocha-Filho, R.C., Saez, C., Cañizares, P., 2012. Influence of
1026 the supporting electrolyte on the electrolyses of dyes with conductive-diamond anodes.
1027 *Chem. Eng. J.* 184, 221–227.
- 1028 Arivoli, S., Thenkuzhali, M., Martin Deva Prasath, P., 2009. Adsorption of rhodamine B by
1029 acid activated carbon- Kinetic, thermodynamic and equilibrium studies. *Orbital* 1 (2), 138-
1030 155.
- 1031 Babuponnusami, A., Muthukumar, K., 2012. Advanced oxidation of phenol: A comparison
1032 between Fenton, electro-Fenton, sono-electro-Fenton and photo-electro-Fenton processes.
1033 *Chem. Eng. J.* 183, 1–9.

- 1034 Bae, J.-S., Freeman, H.S., 2007. Aquatic toxicity evaluation of copper-complexed direct dyes
1035 to the *Daphnia magna*. *Dyes Pigments* 73 (1), 126-132.
- 1036 Bagal, M.V., Gogate, P.R., 2014. Wastewater treatment using hybrid treatment schemes
1037 based on cavitation and Fenton chemistry: A review. *Ultrason.Sonochem.*21 (1), 1–14.
- 1038 Bahnemann, D., 2004. Photocatalytic water treatment: solar energy applications. *Sol. Energy*
1039 77 (5), 445–459.
- 1040 Balci, B., Oturan, M.A., Oturan, N., Sirés, I., 2009. Decontamination of aqueous glyphosate,
1041 (aminomethyl) phosphonic acid, and glufosinate solutions by electro-Fenton-like process
1042 with Mn^{2+} as the catalyst. *J. Agr. Food Chem.*, 57(11), 4888-4894.
- 1043 Barhoumi, N., Labiadh, L., Oturan, M.A., Oturan, N., Gadri, A., Ammar, S., Brillas, E.,
1044 2015. Electrochemical mineralization of the antibiotic levofloxacin by electro-Fenton-
1045 pyrite process. *Chemosphere* 141, 250–257.
- 1046 Barhoumi, N., Oturan, N., Olvera-Vargas, H., Brillas, E., Gadri, A., Ammar, S., Oturan,
1047 M.A., 2016. Pyrite as a sustainable catalyst in electro-Fenton process for improving
1048 oxidation of sulfamethazine. *Kinetics, mechanism and toxicity assessment. Water Res.* 94,
1049 52–61.
- 1050 Barredo-Damas, S., Alcaina-Miranda, M.I., Iborra-Clar, M.I., Bes-Pia, A., Mendoza-Roca,
1051 J.A., Iborra-Clar, A., 2006. Study of the UF process as pretreatment of NF membranes for
1052 textile wastewater reuse. *Desalination* 200 (1-3), 745–747.
- 1053 Bedolla-Guzman, A., Sirés, I., Thiam, A., Peralta-Hernández, J.M., Gutiérrez-Granados, S.,
1054 Brillas, E., 2016. Application of anodic oxidation, electro-Fenton and UVA photoelectro-
1055 Fenton to decolorize and mineralize acidic solutions of Reactive Yellow 160 azo dye.
1056 *Electrochim. Acta* 206, 307–316
- 1057 Benfield, L.D., Weand, B.L., Judkins, J.F., 1982. *Process chemistry for water and wastewater.*
1058 Prentice Hall Inc, Englewood Cliffs, New Jersey.
- 1059 Bensalah, N., Quiroz Alfaro, M.A., Martínez-Huitle, C.A., 2009. Electrochemical treatment
1060 of synthetic wastewaters containing Alphazurine A dye. *Chem. Eng. J.* 149, 348–352.
- 1061 Bogdanowicz, R., Fabiańska, A., Golunski, L., Sobaszek, M., Gnyba, M., Ryl, J., Darowicki,
1062 K., Ossowski, T., Janssens, S.D., Haenen, K., Siedlecka, E.M., 2013, Influence of the
1063 boron doping level on the electrochemical oxidation of the azo dyes at Si/BDD thin film
1064 electrodes. *Diam. Relat. Mater.* 39, 82–88.
- 1065 Braga, N.A., Cairo, C.A.A., Matsushima, J.T., Baldan, M.R., Ferreira, N.G., 2010.
1066 Diamond/porous titanium three-dimensional hybrid electrodes. *J. Solid State Electrochem.*
1067 14, 313-321.
- 1068 Brillas, E., 2014. A Review on the degradation of organic pollutants in waters by UV
1069 photoelectro-Fenton and solar photoelectro-Fenton. *J. Braz. Chem. Soc.* 25 (3), 393-417.
- 1070 Brillas, E., Casado, J., 2002. Aniline degradation by electro-Fenton and peroxi-coagulation
1071 processes using a flow reactor for wastewater treatment. *Chemosphere* 47 (3), 241–248.

- 1072 Brillas, E., Mur, E., Casado, J., 1996. Iron(II) catalysis of the mineralization of aniline using
1073 a carbon-PTFE O₂-fed cathode. *J. Electrochem. Soc.* 143 (3), L49-L53.
- 1074 Brillas, E., Mur, E., Sauleda, R., Sanchez, L., Peral, J., Domenech, X., Casado, J., 1998.
1075 Aniline mineralization by AOP's: anodic oxidation, photocatalysis, electro-Fenton and
1076 photoelectro-Fenton processes. *Appl. Catal. B-Environ.* 16, 31-42.
- 1077 Brillas, E., Sauleda, R., Casado, J., 1997. Peroxi-coagulation of aniline in acidic medium
1078 using an oxygen diffusion cathode. *J. Electrochem. Soc.* 144 (7), 2374 – 2379.
- 1079 Brillas, E., Sauleda, R., Casado, J., 1998. Degradation of 4-chlorophenol by anodic oxidation,
1080 electro-Fenton, photoelectro-Fenton, and peroxi-coagulation processes. *J. Electrochem.*
1081 *Soc.*, 145, 759-765.
- 1082 Canizares, P., Gadri, A., Lobato, J., Nasr, B., Paz, R., Rodrigo, M.A., Saez, C., 2009.
1083 Electrochemical oxidation of azoic dyes with conductive-diamond anodes. *Ind. Eng.*
1084 *Chem. Res.* 45 (10), 3468-3473.
- 1085 Chakma, S., Moholkar, V.S., 2013. Physical mechanism of sono-Fenton process. *AIChE J.* 59
1086 (11), 4303-4313.
- 1087 Chen, G., 2004. Electrochemical technologies in wastewater treatment. *Sep. Purif. Technol.*
1088 38 (1), 11-41.
- 1089 Chen, X., Chen, G., Yue, P.L., 2003. Anodic oxidation of dyes at novel Ti/B-diamond
1090 electrodes. *Chem. Eng. Sci.* 58 (3-6), 995 – 1001.
- 1091 COINDS, 2000. Comprehensive industry documents series on textile industry. Central
1092 Pollution Control Board, India 59, 1999-2000.
- 1093 Comninellis, C., 1994. Electrocatalysis in the electrochemical conversion/combustion of
1094 organic pollutants for waste water treatment. *Electrochim. Acta* 39 (11-12), 1857-1862.
- 1095 Comninellis, C., De Battisti, A., 1996. Electrocatalysis in anodic oxidation of organics with
1096 simultaneous oxygen evolution. *J. Chim. Phys.* 93 (4), 673-679.
- 1097 Compton, R.G., Eklund, J. C., Marken, F., 1997. Sonoelectrochemical Processes: A review.
1098 *Electroanal.* 9 (7), 509-522.
- 1099 Couto, S.R., 2009. Dye removal by immobilised fungi. *Biotechnol. Adv.* 27 (3), 227-235.
- 1100 Crini, G., 2006. Non-conventional low-cost adsorbents for dye removal: A review.
1101 *Bioresource Technol.* 97 (9), 1061-1085.
- 1102 Demirbas, A., 2009. Agricultural based activated carbon for the removal of dyes from
1103 aqueous solutions: A review. *J. Hazard. Mater.* 167 (1-3), 1-9.
- 1104 Diagne, M., Sharma, V.K., Oturan, N., Oturan, M.A., 2014. Depollution of indigo dye by
1105 anodic oxidation and electro-Fenton using B-doped diamond anode. *Environ. Chem. Lett.*
1106 12, 219-224.
- 1107 do Vale-Júnior, E., Dosta, S., Cano, I.G., Guilemany, J.M., Garcia-Segura, S., Martínez-
1108 Huitle, C.A., 2016. Acid blue 29 decolorization and mineralization by anodic oxidation
1109 with a cold gas spray synthesized Sn-Cu-Sb alloy anode. *Chemosphere* 148, 47-54

- 1110 dos Santos, A.J., de Lima, M.D., da Silva, D.R., Garcia-Segura, S., Martínez-Huitle, C.A.,
1111 2016. Influence of the water hardness on the performance of electro-Fenton approach:
1112 Decolorization and mineralization of Eriochrome Black T. *Electrochim. Acta* 208, 156–
1113 163.
- 1114 Drogui, P., Asselin, M., Brar, S.K., Benmoussa, H., Blais, J.F., 2008. Electrochemical
1115 removal of pollutants from agro-industry wastewaters. *Sep. Purif. Technol.* 61 (3), 301–
1116 310.
- 1117 El-Desoky, H.S., Ghoneim, M.M., El-Sheikh, R., Zidan, N.M., 2010. Oxidation of levafix CA
1118 reactive azo-dyes in industrial wastewater of textile dyeing by electro-generated Fenton's
1119 reagent. *J. Hazard. Mater.* 175 (1-3), 858–865.
- 1120 El-Ghenymy, A., Centellas, F., Rodríguez, R.M., Cabot, P.L., Garrido, J.A., Sirés, I., Brillas,
1121 E., 2015. Comparative use of anodic oxidation, electro-Fenton and photoelectro-Fenton
1122 with Pt or boron-doped diamond anode to decolorize and mineralize Malachite Green
1123 oxalate dye. *Electrochim. Acta* 182, 247–256
- 1124 El-Kacemi, S., Zazou, H., Oturan, N., Dietze, M., Hamdani, M., Es-Souni, M., Oturan, M.A.,
1125 2017. Nanostructured ZnO-TiO₂ thin film oxide as anode material in electrooxidation of
1126 organic pollutants. Application to the removal of dye Amido black 10B from water.
1127 *Environ. Sci. Pollut. Res.* 24, 1442-1449.
- 1128 Eslami, A., Moradi, M., Ghanbari, F., Mehdipour, F., 2013. Decolorization and COD
1129 removal from real textile wastewater by chemical and electrochemical Fenton processes: a
1130 comparative study. *J. Environ. Health Sci. Eng.* 11, 31.
- 1131 Faouzi, A.M., Nasr, B., Abdellatif, G., 2007, Electrochemical degradation of anthraquinone
1132 dye Alizarin Red S by anodic oxidation on boron-doped diamond. *Dyes Pigments* 73 (1),
1133 86-89.
- 1134 Feng, C., Li, F., Liu, H., Lang, X., Fan, S., 2010a. A dual-chamber microbial fuel cell with
1135 conductive film-modified anode and cathode and its application for the neutral electro-
1136 Fenton process. *Electrochim. Acta* 55 (6), 2048–2054.
- 1137 Feng, C-H., Li, F-B., Mai, H-J., Li, X-Z., 2010b. Bio-electro-Fenton process driven by
1138 microbial fuel cell for wastewater treatment. *Environ. Sci. Technol.* 44 (5), 1875–1880.
- 1139 Fernández de Dios, M.Á., González del Campo, A., Fernández, F.J., Rodrigo, M., Pazos, M.,
1140 Sanromán, M.Á., 2013. Bacterial–fungal interactions enhance power generation in
1141 microbial fuel cells and drive dye decolourisation by an ex situ and in situ electro-Fenton
1142 process. *Bioresource Technol.* 148, 39–46.
- 1143 Flox, C., Arias, C., Brillas, E., Savall, A., Groenen-Serrano, K., 2009. Electrochemical
1144 incineration of cresols: a comparative study between PbO₂ and boron-doped diamond
1145 anodes. *Chemosphere* 74 (10), 1340–1347.
- 1146 Flox, C., Cabot, P.L., Centellas, F., Garrido, J.A., Rodríguez, R.M., Arias, C., Brillas, E.,
1147 2007a. Solar photoelectro-Fenton degradation of cresols using a flow reactor with a boron-
1148 doped diamond anode. *Appl. Catal. B: Environ.* 75 (1-2), 17-28.

- 1149 Flox, C., Garrido, J.A., Rodríguez, R.M., Cabot, P.L., Centellas, F., Arias, C., Brillas, E.,
1150 2007b. Mineralization of herbicide mecoprop by photoelectro-Fenton with UVA and solar
1151 light. *Catal. Today* 129 (1-2), 29-36.
- 1152 Flox, C., Garrido, J.A., Rodríguez, R.M., Centellas, F., Cabot, P.L., Arias, C., Brillas, E.,
1153 2005. Degradation of 4,6-dinitro-o-cresol from water by anodic oxidation with a boron-
1154 doped diamond electrode. *Electrochim. Acta* 50 (18), 3685–3692.
- 1155 Fu, F., Wang, Q., Tang, B., 2010a. Effective degradation of CI Acid Red 73 by advanced
1156 Fenton process. *J. Hazard. Mater.* 174 (1-3), 17–22.
- 1157 Fu, L., You, S., Yang, F., Gao, M., Fang, X., Zhang, G., 2010b. Synthesis of hydrogen
1158 peroxide in microbial fuel cell. *J. Chem. Technol. Biotechnol.* 85 (5), 715–719.
- 1159 Ganzenko, O., Trelu, C., Papirio, S., Oturan, N., Huguenot, D., van Hullebusch, E.D.,
1160 Esposito, G., Oturan, M.A. (2017). Bioelectro-Fenton: evaluation of a combined
1161 biological-advanced oxidation treatment for pharmaceutical wastewater. *Environ. Sci.*
1162 *Pollut. Res.* (in press), doi: 10.1007/s11356-017-8450-6.
- 1163 Garcia-Segura, S., Brillas, E., 2016. Combustion of textile monoazo, diazo and triazo dyes by
1164 solar photoelectro-Fenton: Decolorization, kinetics and degradation routes. *Appl. Catal. B:*
1165 *Environ.* 181, 681–691
- 1166 Garcia-Segura, S., El-Ghenemy, A., Centellas, F., Rodríguez, R.M., Arias, C., Garrido, J.A.,
1167 Cabot, P.L., Brillas, E., 2012. Comparative degradation of the diazo dye Direct Yellow 4
1168 by electro-Fenton, photoelectro-Fenton and photo-assisted electro-Fenton. *J. Electroanal.*
1169 *Chem.* 681, 36–43.
- 1170 Garcia-Segura, S., Salazar, R., Brillas, E., 2013. Mineralization of phthalic acid by solar
1171 photoelectro-Fenton with a stirred boron-doped diamond/air-diffusion tank reactor:
1172 Influence of Fe³⁺ and Cu²⁺ catalysts and identification of oxidation products. *Electrochim.*
1173 *Acta* 113, 609–619.
- 1174 George, S.J., Gandhimathi, R., Nidheesh, P.V., Ramesh, S.T., 2013. Oxidation of salicylic
1175 acid from aqueous solution with continuous stirred tank reactor by electro-Fenton method.
1176 *Environ. Eng. Sci.* 30 (12), 757-764.
- 1177 George, S.J., Gandhimathi, R., Nidheesh, P.V., Ramesh, S.T., 2014. Electro-Fenton oxidation
1178 of salicylic acid from aqueous solution: Batch studies and degradation pathway. *Clean Soil*
1179 *Air Water* 42(1), 1701-1711.
- 1180 George, S.J., Gandhimathi, R., Nidheesh, P.V., Ramesh, S.T., 2016. Optimization of salicylic
1181 acid removal by electro Fenton process in a continuous stirred tank reactor using response
1182 surface methodology. *Desalination Water Treat.* 57, 4234–4244.
- 1183 Ghoneim, M.M., El-Desoky, H.S., Zidan, N.M., 2011. Electro-Fenton oxidation of Sunset
1184 Yellow FCF azo-dye in aqueous solutions. *Desalination* 274 (1-3), 22–30.
- 1185 Ghosh, P., Thakur, L.K., Samanta, A.N., Ray, S., 2012. Electro-Fenton treatment of synthetic
1186 organic dyes: Influence of operational parameters and kinetic study. *Korean J. Chem. Eng.*
1187 29 (9), 1203-1210.

- 1188 Girish Kumar, S., Gomathi Devi, L., 2011. Review on modified TiO₂ photocatalysis under
1189 UV/visible light: Selected results and related mechanisms on interfacial charge carrier
1190 transfer dynamics. *J. Phys. Chem. A* 115 (46), 13211–13241.
- 1191 Gogate, P.R., Pandit, A.B., 2004. A review of imperative technologies for wastewater
1192 treatment II: Hybrid methods. *Adv. Environ. Res.* 8 (3-4), 553–597.
- 1193 Gogate, P.R., Tatake, P.A., Kanthale, P.M., Pandit, A.B., 2002. Mapping of sonochemical
1194 reactors: Review, analysis, and experimental verification. *AIChE J.* 48 (7), 1542-1560.
- 1195 Gong, R., Jin, Y., Chen, J., Hu, Y., Sun, J., 2007. Removal of basic dyes from aqueous
1196 solution by sorption on phosphoric acid modified rice straw. *Dyes Pigments* 73 (3), 332–
1197 337.
- 1198 Gong, Y., Radachowsky, S.E., Wolf, M., Nielsen, M.E., Girguis, P.R., Reimers, C.E., 2011.
1199 Benthic microbial fuel cell as direct power source for an acoustic modem and seawater
1200 oxygen/temperature sensor system. *Environ. Sci. Technol.* 45 (11), 5047–5053.
- 1201 Goodridge, F., Scott, K., 1994. *Electrochemical Process Engineering*, Plenum Press, New
1202 York.
- 1203 Gözmen, B., Kayan, B., Murat Gizir, A., Hesenov, A., 2009. Oxidative degradations of
1204 reactive blue 4 dye by different advanced oxidation methods. *J. Hazard. Mater.* 168 (1),
1205 129–136.
- 1206 Guivarch, E., Oturan M.A., 2004. The problem of the contamination of waters by synthetic
1207 dyes: how to destroy them? Application of the electro-Fenton process. *Actual. Chimique*
1208 277-278, 65-69.
- 1209 Guivarch, E., Trévin, S., Lahitte, C., Oturan M.A., 2003. Degradation of azo dyes in water by
1210 electro-Fenton process. *Environ. Chem. Lett.* 1(1), 39-44.
- 1211 Gupta, N., Oloman, C.W., 2006. Scale-up of the perforated bipole trickle-bed electrochemical
1212 reactor for the generation of alkaline peroxide. *J. Appl. Electrochem.* 36, 1133–1141.
- 1213 Haidar, M., Dirany, A., Sirés, I., Oturan, N., Oturan, M.A., 2013. Electrochemical
1214 degradation of the antibiotic sulfachloropyridazine by hydroxyl radicals generated at a
1215 BDD anode. *Chemosphere* 91 (9), 1304–1309.
- 1216 Hammami, S., Oturan, N., Bellakhal, N., Dachraoui, M., Oturan, M.A. 2007. Oxidative
1217 degradation of direct orange 61 by electro-Fenton process using a carbon felt electrode:
1218 Application of the experimental design methodology. *J. Electroanal. Chem.* 610 (1), 75–
1219 84.
- 1220 Hu, Z., Zhou, M., Zhou, L., Li, Y., Zhang, C. 2014. Effect of matrix on the electrochemical
1221 characteristics of TiO₂ nanotube arrays based PbO₂ electrode for pollutant degradation.
1222 *Environ. Sci. Pollut. Res.* 21, 8476–8484.
- 1223 Iglesias, O., Fernández de Dios, M.A., Pazos, M., Sanromán, M.A., 2013a. Using iron-loaded
1224 sepiolite obtained by adsorption as a catalyst in the electro-Fenton oxidation of Reactive
1225 Black 5. *Environ. Sci. Pollut. Res.* 20 (9), 5983-5993.

- 1226 Iglesias, O., Rosales, E., Pazos, M., Sanromán, M.A., 2013b. Electro-Fenton decolourisation
1227 of dyes in an airlift continuous reactor using iron alginate beads. *Environ. Sci. Pollut. Res.*
1228 20 (4), 2252–2261.
- 1229 Iranifam, M., Zarei, M., Khataee, A.R., 2011. Decolorization of C.I. Basic Yellow 28
1230 solution using supported ZnO nanoparticles coupled with photoelectro-Fenton process. *J.*
1231 *Electroanal. Chem.* 659 (1), 107–112.
- 1232 Isarain-Chávez, E., de la Rosa, C., Martínez-Huitle, C.A., Peralta-Hernández, J.M., 2013. On-
1233 site hydrogen peroxide production at pilot flow plant: Application to electro-Fenton
1234 process. *Int. J. Electrochem. Sci.* 8, 3084 – 3094.
- 1235 Ji, F., Li, C., Zhang, J., Deng, L., 2011. Efficient decolorization of dye pollutants with
1236 $\text{LiFe}(\text{WO}_4)_2$ as a reusable heterogeneous Fenton-like catalyst. *Desalination* 269 (1-3),
1237 284–290.
- 1238 Ju, D.J., Byun, I.G., Park, J.J., Lee, C.H., Ahn, G.H., Park, T.J., 2008. Biosorption of a
1239 reactive dye (Rhodamine-B) from an aqueous solution using dried biomass of activated
1240 sludge. *Bioresour. Technol.* 99 (17), 7971–7975.
- 1241 Jüttner, K., Galla, U., Schmieder, H., 2000. Electrochemical approaches to environmental
1242 problems in the process industry. *Electrochim. Acta* 45 (15-16), 2575–94.
- 1243 Karthikeyan, S., Jambulingam, M., Sivakumar, P., Shekhar, A.P., Krithika, J., 2006. Impact
1244 of textile effluents on fresh water fish *Mastacembelus Armatus* (Cuv.& Val). *E-J. Chem.* 3
1245 (4), 303-306.
- 1246 Kavitha, V., Palanivelu, K., 2004. The role of ferrous ion in Fenton and photo-Fenton
1247 processes for the degradation of phenol. *Chemosphere* 55 (9), 1235–1243
- 1248 Kayan, B., Gözmen, B., Demirel, M., Murat Gizir, A., 2010. Degradation of acid red 97 dye
1249 in aqueous medium using wet oxidation and electro-Fenton techniques. *J. Hazard.*
1250 *Mater.* 177 (1-3), 95–102.
- 1251 Khataee, A.R., Vahid, B., Behjati, B., Safarpour, M., Joo, S.W., 2014. Kinetic modeling of a
1252 triarylmethane dye decolorization by photoelectro-Fenton process in a recirculating
1253 system: Nonlinear regression analysis. *Chem. Eng. Res. Des.* 92 (2), 362–367.
- 1254 Khataee, A.R., Vatanpour, V., Amani Ghadim, A.R., 2009. Decolorization of C.I. Acid Blue
1255 9 solution by UV/nano-TiO₂, Fenton, Fenton-like, electro-Fenton and electrocoagulation
1256 processes: a comparative study. *J. Hazard. Mater.* 161 (2-3), 1225–1233.
- 1257 Khataee, A.R., Zarei, M., 2011. Photocatalysis of a dye solution using immobilized ZnO
1258 nanoparticles combined with photoelectrochemical process. *Desalination* 273 (2-3), 453–
1259 460.
- 1260 Khataee, A.R., Zarei, M., Asl, S.K., 2010b. Photocatalytic treatment of a dye solution using
1261 immobilized TiO₂ nanoparticles combined with photoelectro-Fenton process:
1262 Optimization of operational parameters. *J. Electroanal. Chem.* 648 (2), 143–150.

- 1263 Khataee, A.R., Zarei, M., Moradkhannejhad, L., 2010a. Application of response surface
1264 methodology for optimization of azo dye removal by oxalate catalyzed photoelectro-
1265 Fenton process using carbon nanotube-PTFE cathode. *Desalination* 258 (1-3), 112–119.
- 1266 Klemola, K., Honkalampi-Hämäläinen, U., Liesivuori, J., Pearson, J., Lindström-Seppä, P.,
1267 2006. Evaluating the toxicity of reactive dyes and fabrics with the spermatozoa motility
1268 inhibition test. *Autex Res. J.* 6 (3), 182-190.
- 1269 Klemola, K., Pearson, J., Lindstrom-Seppä, P., 2007. Evaluating the toxicity of reactive dyes
1270 and dyed fabrics with the HaCaT cytotoxicity test. *Autex Res. J.* 7 (3), 217-223.
- 1271 Kwon, B.G., Lee, D.S., Kang, N., Yoon, J., 1999. Characteristics of p-chlorophenol oxidation
1272 by Fenton's reagent. *Water Res.* 33 (9), 2110-2118.
- 1273 Labiadh, L., Oturan, M.A., Panizza, M., Ben Hamadi, N., Ammar, S., 2015. Complete
1274 removal of AHPS synthetic dye from water using new electro-Fenton oxidation catalyzed
1275 by natural pyrite as heterogeneous catalyst. *J. Hazard. Mater.* 297, 34-41
- 1276 Labiadh, L., Barbucci, A., Carpanese, M.P., Gadri, A., Ammar, S., Panizza, M., 2016.
1277 Comparative depollution of Methyl Orange aqueous solutions by electrochemical
1278 incineration using TiRuSnO₂, BDD and PbO₂ as high oxidation power anodes. *J.*
1279 *Electroanal. Chem.* 766, 94–99.
- 1280 Lahkimi, A., Oturan, M.A., Oturan, N., Chaouch, M., 2007. Removal of textile dyes from
1281 water by the electro-Fenton process. *Environ. Chem. Lett.* 5, 35–39.
- 1282 Lam, S-M., Sin, J-C., Abdullah, A.Z., Mohamed, A.R., 2012. Degradation of wastewaters
1283 containing organic dyes photocatalysed by zinc oxide: A review. *Desalination Water*
1284 *Treat.* 41 (1-3), 131–169.
- 1285 Le, T.X.H., Bechelany, M., Lacour, S., Oturan, N., Oturan, M.A., Cretin, M., 2015. High
1286 removal efficiency of dye pollutants by electron-Fenton process using a graphene based
1287 cathode. *Carbon* 94, 1003–1011
- 1288 Le, T.X.H., Nguyen, T.V., Yacouba, Z.A., Zoungrana, L., Avril, F., Petit, E., Mendret, J.,
1289 Bonniol, V., Bechelany, M., Lacour, S., Lesage, G., Cretin, M., 2016. Toxicity removal
1290 assessments related to degradation pathways of azo dyes: Toward an optimization of
1291 Electro-Fenton treatment. *Chemosphere* 161, 308-318
- 1292 Li, H., Lei, H., Yu, Q., Li, Z., Feng, X., Yang, B., 2010b. Effect of low frequency ultrasonic
1293 irradiation on the sonoelectro-Fenton degradation of cationic red X-GRL. *Chem. Eng. J.*
1294 160 (2), 417–422.
- 1295 Li, H., Zhu, X., Ni, J., 2010a. Inactivation of *Escherichia coli* in Na₂SO₄ electrolyte using
1296 boron-doped diamond anode. *Electrochim. Acta* 56 (1), 448–453.
- 1297 Liang, L, An, Y.R., Yu, F.K., Liu, M.M, Ren, G.B., Zhou, M.H. 2016. Novel rolling-made
1298 gas-diffusion electrode loading trace transition metal for efficient heterogeneous electro-
1299 Fenton-like. *J. Environ. Chem. Eng.* 4, 4400-4408.

- 1300 Lin, H., Zhang, H., Wang, X., Wang, L., Wu, J., 2014. Electro-Fenton removal of Orange II
1301 in a divided cell: Reaction mechanism, degradation pathway and toxicity evolution. *Sep.*
1302 *Purif. Technol.* 122, 533–540.
- 1303 Liu, X-W., Sun, X-F., Li, D-B., Li, W-W., Huang, Y-X., Sheng, G-P., Yu, H-Q., 2012.
1304 Anodic Fenton process assisted by a microbial fuel cell for enhanced degradation of
1305 organic pollutants. *Water Res.* 46 (14), 4371-4378.
- 1306 Lounis, M., Samar, M.E., Hamdaoui, O., 2016. Sono-electrochemical degradation of Orange
1307 G in pure water, natural water, and seawater: effect of operating parameters. *Desalination*
1308 *Water Treat.* 57(47), 22533-22542
- 1309 Ma, L., Zhou, M.H., Ren, G.B., Yang, W.L., Liang, L., 2016. A highly energy-efficient flow-
1310 through electro-Fenton process for organic pollutants degradation. *Electrochim. Acta* 200,
1311 222-230
- 1312 Magario, I., García Einschlag, F.S., Rueda, E.H., Zygadlo, J., Ferreira, M.L., 2012.
1313 Mechanisms of radical generation in the removal of phenolderivatives and pigments using
1314 different Fe-based catalytic systems. *J. Mol. Catal. A: Chem.*352, 1-20.
- 1315 Malik, P.K., 2003. Use of activated carbons prepared from sawdust and rice-husk for
1316 adsorption of acid dyes: a case study of Acid Yellow 36. *Dyes Pigments* 56 (3), 239–249.
- 1317 Mane, V.S., Mall, I.D., Srivastava, V.C., 2007. Use of bagasse fly ash as an adsorbent for the
1318 removal of brilliant green dye from aqueous solution. *Dyes Pigments* 73 (3), 269–278.
- 1319 Martínez, S.S., Uribe, E.V., 2012. Enhanced sonochemical degradation of azure B dye by the
1320 electroFenton process. *Ultrason.Sonochem.*19 (1), 174–178.
- 1321 Martínez-Huitle, C.A., Brillas, E., 2009.Decontamination of wastewaters containing synthetic
1322 organic dyes by electrochemical methods: A general review. *Appl. Catal. B: Environ.* 87
1323 (3-4), 105–145.
- 1324 Martínez-Huitle, C.A., dos Santos, E.V., de Araújo, D.M., Panizza, M., 2012. Applicability
1325 of diamond electrode/anode to the electrochemical treatment of areal textile effluent. *J.*
1326 *Electroanal. Chem.* 674, 103–107.
- 1327 Mathur, N., Bhatnagar, P., Bakre, P., 2005. Assessing mutagenicity of textile dyes from pali
1328 (Rajasthan) using ames bioassay. *Appl. Ecology Environ. Res.* 4 (1), 111-118.
- 1329 Medvedev, Z.A., Crowne, H.M., Medvedeva, M.N., 1988. Age related variations of hepato
1330 carcinogenic effect of azo dye (3'-MDAB) as linked to the level of hepatocyte
1331 polyploidization. *Mech. Ageing Dev.* 46 (1-3), 159-174.
- 1332 Migliorini, F.L., Braga, N.A., Alves, S.A., Lanza, M.R.V., Baldan, M.R., Ferreira, N.G.,
1333 2011. Anodic oxidation of wastewater containing the Reactive Orange 16 Dye using
1334 heavily boron-doped diamond electrodes. *J. Hazard. Mater.*192 (3), 1683–1689.
- 1335 Miled, W., Said, A., Roudseli, S., 2010. Decolorization of high polluted textile wastewater by
1336 indirect electrochemical oxidation process. *JTATM* 6 (3), 1-6.

- 1337 Moreira, F.C., Garcia-Segura, S., Vilar, V.J.P., Boaventura, R.A.R., Brillas, E., 2013.
1338 Decolorization and mineralization of Sunset Yellow FCF azo dye by anodic oxidation,
1339 electro-Fenton, UVA photoelectro-Fenton and solar photoelectro-Fenton processes. *Appl.*
1340 *Catal. B: Environ.* 142, 877-890.
- 1341 Murati, M., Oturan, N., Aaron, J.-J., Dirany, A., Tassin, B., Zdravkovski, Z., Oturan, M.A.,
1342 2012. Degradation and mineralization of sulcotrione and mesotrione in aqueous medium
1343 by the electro-Fenton process: a kinetic study. *Environ. Sci. Pollut. Res.* 19 (5), 1563–
1344 1573.
- 1345 Muruganandham, M., Swaminathan, M., 2004. Decolourisation of Reactive Orange 4 by
1346 Fenton and photo-Fenton oxidation technology. *Dyes Pigments* 63 (3), 315-321
- 1347 Muruganathan, M., Yoshihara, S., Rakuma, T., Uehara, N., Shirakashi, T., 2007.
1348 Electrochemical degradation of 17 β -estradiol (E2) at boron-doped diamond (Si/BDD) thin
1349 film electrode. *Electrochim. Acta* 52 (9), 3242–3249.
- 1350 Namasivayam, C., Kavitha, D., 2002. Removal of Congo Red from water by adsorption onto
1351 activated carbon prepared from coir pith, an agricultural solid waste. *Dyes Pigments* 54
1352 (1), 47–58.
- 1353 Nava, J.L., Quiroz, M.A., Martínez-Huitle, C.A., 2008. Electrochemical treatment of
1354 synthetic wastewaters containing alaphazurine A dye: Role of Electrode material in the
1355 colour and cod removal. *J. Mex. Chem. Soc.* 52 (4), 249-255.
- 1356 Neyens, E., Baeyens, J., 2003. A review of classic Fenton's peroxidation as an advanced
1357 oxidation technique. *J. Hazard. Mater.* B98 (1-3), 33–50.
- 1358 Nidheesh, P.V., 2015. Heterogeneous Fenton catalysts for the abatement of organic pollutants
1359 from aqueous solution: a review. *RSC Adv.* 5, 40552–40577.
- 1360 Nidheesh, P.V., Gandhimathi, R., 2012. Trends in electro-Fenton process for water and
1361 wastewater treatment: An overview. *Desalination* 299, 1–15.
- 1362 Nidheesh, P.V., Gandhimathi, R., 2014a. Removal of rhodamine B from aqueous solution
1363 using graphite- graphite electro Fenton system. *Desalination Water Treat.* 52, 1872–1877.
- 1364 Nidheesh, P.V., Gandhimathi, R., 2014b. Comparative removal of rhodamine B from aqueous
1365 solution by electro Fenton and electro Fenton like processes. *Clean- Soil, Air, Water.*
1366 42(6), 779-784.
- 1367 Nidheesh, P.V., Gandhimathi, R., 2014c. Effect of solution pH on the performance of three
1368 electrolytic advanced oxidation processes for the treatment of textile wastewater and
1369 sludge characteristics. *RSC Adv.* 4, 27946–27954.
- 1370 Nidheesh, P.V., Gandhimathi, R., 2014d. Electrolytic removal of Rhodamine B from aqueous
1371 solution by peroxicoagulation process. *Environ. Sci. Pollut. Res.* 21, 8585–8594.
- 1372 Nidheesh, P.V., Gandhimathi, R., 2015a. Electro Fenton oxidation for the removal of
1373 Rhodamine B from aqueous solution in a bubble column reactor under continuous mode.
1374 *Desalination Water Treat.* 55, 263-273.

- 1375 Nidheesh, P.V., Gandhimathi, R., 2015b. Textile Wastewater Treatment by Electro-Fenton
1376 Process in Batch and Continuous Modes. *J. Hazard. Toxic Radioact. Waste* 19(3),
1377 04014038.
- 1378 Nidheesh, P.V., Gandhimathi, R., Ramesh, S.T., 2013. Degradation of dyes from aqueous
1379 solution by Fenton processes: A Review. *Environ. Sci. Pollut. Res.* 20, 2099–2132.
- 1380 Nidheesh, P.V., Gandhimathi, R., Sanjini, N.S., 2014b. NaHCO₃ enhanced Rhodamine B
1381 removal from aqueous solution by graphite–graphite electro Fenton system. *Sep. Purif.*
1382 *Technol.* 132, 568-576.
- 1383 Nidheesh, P.V., Gandhimathi, R., Velmathi, S., Sanjini, N.S., 2014a. Magnetite as a
1384 heterogeneous electro Fenton catalyst for the removal of Rhodamine B from aqueous
1385 solution. *RSC Adv.* 4, 5698-5708.
- 1386 Olvera-Vargas, H., Cocerva, T., Oturan, N., Buisson, D., Oturan, M.A., 2016a. Bioelectro-
1387 Fenton: A sustainable integrated process for removal of organic pollutants from water:
1388 Application to mineralization of metoprolol. *Journal of Hazardous Materials* 319 (2016)
1389 13–23.
- 1390 Olvera-Vargas, H., Oturan, N., Buisson, D., Oturan, M.A., 2016b. A coupled Bio-EF process
1391 for mineralization of the pharmaceuticals Furosemide and Ranitidine: feasibility
1392 assessment. *Chemosphere*, 155, 606-613.
- 1393 Olvera-Vargas, H., Oturan, N., Aravindakumar, C.T., Sunil Paul, M.M., Sharma, V.K.,
1394 Oturan, M.A., 2014. Electro-oxidation of the dye azure B: kinetics, mechanism, and by-
1395 products. *Environ. Sci. Pollut. Res.* 21, 8379-8386.
- 1396 Oturan, M.A. Pinson, J., 1995. Hydroxylation by electrochemically generated •OH radicals.
1397 Mono- and polyhydroxylation of benzoic acid: products and isomers' distribution. *J. Phys.*
1398 *Chem.* 99(38), 13948-13954.
- 1399 Oturan, M.A., 2000. An ecologically effective water treatment technique using
1400 electrochemically generated hydroxyl radicals for in situ destruction of organic pollutants:
1401 Application to herbicide 2,4-D. *J. Appl. Electrochem.* 30, 475-482.
- 1402 Oturan, M.A., Aaron, J.-J., 2014. Advanced oxidation processes in water/wastewater
1403 treatment: Principles and applications. A review. *Crit. Rev. Env. Sci. Technol.* 44, 2577-
1404 2641.
- 1405 Oturan, M.A., Edelahi, M.C., Oturan, N., El Kacemi, K., Aaron, J.-J., 2010a. Kinetics of
1406 oxidative degradation/mineralization pathways of the phenylurea herbicides diuron,
1407 monuron and fenuron in water during application of the electro-Fenton process. *Appl.*
1408 *Catal. B: Environ.* 97 (1-2), 82–89.
- 1409 Oturan, M.A., Guivarch, E., Oturan, N., Sirés, I., 2008a. Oxidation pathways of malachite
1410 green by Fe³⁺-catalyzed electro-Fenton process. *Appl. Catal. B: Environ.* 82 (3-4), 244–
1411 254.

- 1412 Oturan, M.A., Oturan, N., Lahitte, C., Trevin, S., 2001. Production of hydroxyl radicals by
1413 electrochemically assisted Fenton's reagent. Application to the mineralization of an
1414 organic micropollutant, the pentachlorophenol. *J. Electroanal. Chem.*, 507 (1-2), 96-102.
- 1415 Oturan, M.A., Peirotten, J., Chartrin, P., Acher, A.J., 2000. Complete destruction of p-
1416 Nitrophenol in aqueous medium by electro-Fenton method. *Environ. Sci. Technol.* 34
1417 (16), 3474-3479.
- 1418 Oturan, M.A., Sirés, I., Oturan, N., Pérocheau, S., Laborde, J-L., Trévin, S., 2008b.
1419 Sono-electro-Fenton process: A novel hybrid technique for the destruction of organic
1420 pollutants in water. *J. Electroanal. Chem.* 624 (1-2), 329-332.
- 1421 Oturan, M.A., Oturan, N., Aaron, J.-J., 2004. Treatment of organic micropollutants in aqueous
1422 medium by advanced oxidation process. *Actual. Chimique* 277-278, 57-64
- 1423 Oturan, N., Brillas, E., Oturan, M.A., 2012. Unprecedented total mineralization of atrazine
1424 and cyanuric acid by anodic oxidation and electro-Fenton with a boron-doped diamond
1425 anode. *Environ. Chem. Lett.*, 10(2), 165-170.
- 1426 Oturan, N., Zhou, M., Oturan, M.A., 2010b. Metomyl Degradation by electro-Fenton and
1427 electro-Fenton-like processes: A kinetics study of the effect of the nature and
1428 concentration of some transition metal ions as catalyst. *J. Phys. Chem. A* 114 (39), 10605-
1429 10611.
- 1430 Özcan, A., Oturan, M.A., Oturan, N., Sahin, Y., 2009b. Removal of Acid Orange 7 from
1431 water by electrochemically generated Fenton's reagent. *J. Hazard. Mater.* 163 (2-3), 1213-
1432 1220.
- 1433 Özcan, A., Sahin, Y., Oturan, M.A., 2008b. Removal of prophan from water by using
1434 electro-Fenton technology: Kinetics and mechanism. *Chemosphere* 73 (5), 737-744.
- 1435 Özcan, A., Sahin, Y., Oturan, M.A., 2013. Complete removal of the insecticide azinphos
1436 methyl from water by the electro-Fenton method A kinetic and mechanistic study. *Water*
1437 *Res.* 47 (3), 1470-1479.
- 1438 Özcan, A., Sahin, Y., Koparal, A.S., Oturan, M.A., 2008a. Prophan mineralization in
1439 aqueous medium by anodic oxidation using boron-doped diamond anode: Influence of
1440 experimental parameters on degradation kinetics and mineralization efficiency. *Water Res.*
1441 42 (12), 2889-2898.
- 1442 Özcan, A., Sahin, Y., Koparal, A.S., Oturan, M.A., 2009a. A comparative study on the
1443 efficiency of electro-Fenton process in the removal of prophan from water. *Appl. Catal.*
1444 *B: Environ.* 89 (3-4), 620-626.
- 1445 Özcan, A., Sahin, Y., Koparal A.S., Oturan, M.A., 2008c. Carbon sponge as a new cathode
1446 material for the electro-Fenton process: Comparison with carbon felt cathode and
1447 application to degradation of synthetic dye basic blue 3 in aqueous medium. *J. Electroanal.*
1448 *Chem.* 616 (1-2), 71-78.

- 1449 Panizza, M., Barbucci, A., Ricotti, R., Cerisola, G., 2007. Electrochemical degradation of
1450 methylene blue. *Sep. Purif. Technol.* 54, 382–387.
- 1451 Panizza, M., Cerisola, G., 2001. Removal of organic pollutants from industrial wastewater by
1452 electrogenerated Fenton's reagent. *Water Res.* 35 (16), 3987–3992.
- 1453 Panizza, M., Cerisola, G., 2008. Electrochemical degradation of methyl red using BDD and
1454 PbO₂ anodes. *Ind. Eng. Chem. Res.* 47 (18), 6816–6820.
- 1455 Panizza, M., Cerisola, G., 2009. Direct and mediated anodic oxidation of organic pollutants.
1456 *Chem. Rev.*, 109 (2009) 6541–6569.
- 1457 Panizza, M., Oturan, M.A., 2011. Degradation of Alizarin Red by electro-Fenton process
1458 using a graphite-felt cathode. *Electrochim. Acta* 56 (20), 7084–7087.
- 1459 Peralta-Hernández, J.M., Martínez-Huitile, C.A., Guzmán-Mar, J.L., Hernández-Ramírez, A.,
1460 2009. Recent advances in the application of electro-Fenton and photoelectro-Fenton
1461 process for removal of synthetic dyes in wastewater treatment. *J. Environ. Eng. Manage.*
1462 19 (5), 257–265.
- 1463 Peralta-Hernández, J.M., Meas-Vong, Y., Rodríguez, F.J., Chapman, T.W., Maldonado, M.I.,
1464 Godínez, L.A., 2008. Comparison of hydrogen peroxide-based processes for treating dye-
1465 containing wastewater: Decolorization and destruction of Orange II azo dye in dilute
1466 solution. *Dyes Pigments* 76 (3), 656–662.
- 1467 Percy, A.J., Moore, N., Chipman, J.K., 1989. Formation of nuclear anomalies in rat intestine
1468 by benzidine and its biliary metabolites. *Toxicol.* 57 (2), 217–223.
- 1469 Petrucci, E., Montanaro, D., 2011. Anodic oxidation of a simulated effluent containing
1470 Reactive Blue 19 on a boron-doped diamond electrode. *Chem. Eng. J.* 174 (2-3), 612–618.
- 1471 Pignatello, J.J.; Oliveros, E., Mackay, A., 2006. Advanced oxidation processes for organic
1472 contaminant destruction based on the Fenton reaction and related chemistry. *Crit. Rev.*
1473 *Environ. Sci. Technol.* 36 (1), 1–84.
- 1474 Ponnusami, V., Vikram, S., Srivastava, S.N., 2008. Guava (*Psidium guajava*) leaf powder:
1475 Novel adsorbent for removal of methylene blue from aqueous solutions. *J. Hazard.*
1476 *Mater.* 152 (1), 276–286.
- 1477 Pradhan, A.A., Gogate, P.R., 2010. Degradation of p-nitrophenol using acoustic cavitation
1478 and Fenton chemistry. *J. Hazard. Mater.* 173 (1-3), 517–522.
- 1479 Rabaey, K., Rozendal, R.A., 2010. Microbial electrosynthesis- revisiting the electrical route
1480 for microbial production. *Nature Rev. Microbiol.* 8, 706–716.
- 1481 Ramachandran, R., Saraswathi, R., 2011. Sonoelectrochemical studies on mass transport in
1482 some standard redox systems. *Russ. J. Electrochem.* 47 (1), 15–25.
- 1483 Ramírez, C., Saldana, A., Hernández, B., Acero, R., Guerra, R., Garcia-Segura, S., Brillas, E.,
1484 Peralta-Hernández, J.M., 2013. Electrochemical oxidation of methyl orange azo dye at
1485 pilot flow plant using BDD technology. *J. Ind. Eng. Chem.* 19 (2), 571–579.

- 1486 Rauf, M.A., Meetani, M.A., Hisaindee, S., 2011. An overview on the photocatalytic
1487 degradation of azo dyes in the presence of TiO₂ doped with selective transition metals.
1488 *Desalination* 276 (1-3), 13–27.
- 1489 Ren, G.B., Zhou, M.H., Liu, M.M., Ma, L., Yang, H.J., 2016. A novel vertical-flow electro-
1490 Fenton reactor for organic wastewater treatment. *Chem. Eng. J.* 298, 55-67.
- 1491 Rodriguez, J., Rodrigo, M.A., Panizza, M., Cerisola, G., 2009. Electrochemical oxidation of
1492 Acid Yellow 1 using diamond anode. *J. Appl. Electrochem.* 39 (11), 2285-2289.
- 1493 Rosales, E., Iglesias, O., Pazos, M., Sanromán, M.A., 2012. Decolourisation of dyes under
1494 electro-Fenton process using Fe alginate gel beads. *J. Hazard. Mater.* 213– 214, 369–377.
- 1495 Roshini, P.S., Gandhimathi, R., Ramesh, S.T., Nidheesh, P.V., 2018. Combined electro-
1496 Fenton and biological processes for the treatment of industrial textile effluent:
1497 Mineralization and toxicity analysis. *J. Hazard. Toxic Radioact. Waste* 21(4), doi:
1498 10.1061/(ASCE)HZ.2153-5515.0000370
- 1499 Ruiz, E.J., Arias, C., Brillas, E., Hernández-Ramírez, A., Peralta-Hernández, J.M., 2011b.
1500 Mineralization of Acid Yellow 36 azo dye by electro-Fenton and solar photoelectro-
1501 Fenton processes with a boron-doped diamond anode. *Chemosphere* 82 (4), 495–501.
- 1502 Ruiz, E.J., Hernández-Ramírez, A., Peralta-Hernández, J.M., Arias, C., Brillas, E., 2011a.
1503 Application of solar photoelectro-Fenton technology to azo dyes mineralization: Effect of
1504 current density, Fe²⁺ and dye concentrations. *Chem. Eng. J.* 171 (2), 385– 392.
- 1505 Saez, C., Panizza, M., Rodrigo, M.A., Cerisola, G., 2007. Electrochemical incineration of
1506 dyes using a boron-doped diamond anode. *J. Chem. Technol. Biot.* 82 (6), 575-581.
- 1507 Şahinkaya, S., 2013. COD and color removal from synthetic textile wastewater by ultrasound
1508 assisted electro-Fenton oxidation process. *J. Ind. Eng. Chem.* 19 (2), 601–605.
- 1509 Salari, D., Niaei, A., Khataee A., Zarei, M., 2009. Electrochemical treatment of dye solution
1510 containing C.I. basic yellow 2 by the peroxi-coagulation method and modeling of
1511 experimental results by artificial neural networks. *J. Electroanal. Chem.* 629 (1-2), 117–
1512 125.
- 1513 Salazar, R., Garcia-Segura, S., Ureta-Zañartu, M.S., Brillas, E., 2011. Degradation of
1514 disperse azo dyes from water by solar photoelectro-Fenton. *Electrochim. Acta* 56 (18),
1515 6371–6379.
- 1516 Salazar, R., Ureta-Zañartu, M.S., 2012. Degradation of acid violet 7 and reactive black 5 in
1517 water by electro-Fenton and photo electro-Fenton. *J. Chil. Chem. Soc.* 57 (1), 999-1003.
- 1518 Saltmiras, D.A., Lemley, A.T., 2000. Degradation of ethylene thiourea (ETU) with three
1519 Fenton treatment processes. *J. Agric. Food Chem.* 48 (12), 6149–6157.
- 1520 Sandhya, S., Sarayu, K., Swaminathan, K., 2008. Determination of kinetic constants of hybrid
1521 textile wastewater treatment system. *Bioresource Technol.* 99 (13), 5793–5797.

- 1522 Scialdone, O., 2009. Electrochemical oxidation of organic pollutants in water at metal oxide
1523 electrodes: A simple theoretical model including direct and indirect oxidation processes at
1524 the anodic surface. *Electrochim. Acta* 54 (26), 6140–6147.
- 1525 Scialdone, O., Galia, A., Sabatino, S., 2013. Electro-generation of H₂O₂ and abatement of
1526 organic pollutant in water by an electro-Fenton process in a microfluidic
1527 reactor. *Electrochem. Commun.* 26, 45–47.
- 1528 Sekar, P., Hari Prasad, S., Decca Raman, M., 2009. Effect of textile dye industry effluent on
1529 the nutritive value of fresh water female crab *Spiralothelphusa hydrodroma* (Herbst). *J.*
1530 *Appl. Sci. Res.* 5 (11), 2041-2048.
- 1531 Siddique, M., Farooq, R., Khan, Z.M., Khan, Z., Shaukat, S.F., 2011. Enhanced
1532 decomposition of reactive blue 19 dye in ultrasound assisted electrochemical reactor.
1533 *Ultrason. Sonochem.* 18 (1), 190–196.
- 1534 Sirés, I., Brillas, E., Oturan, M.A., Rodrigo, M.A., Panizza, M., 2014. Electrochemical
1535 advanced oxidation processes: today and tomorrow. A review. *Environ. Sci. Pollut. Res.*
1536 21, 8336-8367.
- 1537 Sirés, I., Cabot, P.L., Centellas, F., Garrido, J.A., Rodríguez, R.M., Arias, C., Brillas, E.,
1538 2006. Electrochemical degradation of clofibrac acid in water by anodic oxidation
1539 Comparative study with platinum and boron-doped diamond electrodes. *Electrochim. Acta*
1540 52 (1), 75–85.
- 1541 Sirés, I., Guivarch, E., Oturan, N., Oturan, M.A., 2008. Efficient removal of
1542 triphenylmethane dyes from aqueous medium by in situ electrogenerated Fenton's reagent
1543 at carbon-felt cathode. *Chemosphere* 72 (4), 592–600.
- 1544 Sivasankar, T., Moholkar, V.S., 2010. Physical insight into the sonochemical degradation of
1545 2,4-dichlorophenol. *Environ. Technol.* 31 (14), 1483–1494.
- 1546 Solano, A.M.S., Garcia-Segura, S., Martínez-Huitle, C.A., Brillas, E., 2015. Degradation of
1547 acidic aqueous solutions of the diazo dye Congo Red by photo-assisted electrochemical
1548 processes based on Fenton's reaction chemistry. *Appl. Catal. B: Environ.* 168-169, 559–
1549 571
- 1550 Song, S., Fan, J., He, Z., Zhan, L., Liu, Z., Chen, J., Xu, X., 2010. Electrochemical
1551 degradation of azo dye C.I. Reactive Red 195 by anodic oxidation on Ti/SnO₂–Sb/PbO₂
1552 electrodes. *Electrochim. Acta* 55 (11), 3606–3613.
- 1553 Sopaj F., Rodrigo M.A., Oturan N., Podvorica F.I., Pinson J., Oturan M.A., 2015. Influence
1554 of the anode materials on the electrochemical oxidation efficiency. Application to
1555 oxidative degradation of the pharmaceutical amoxicillin. *Chem. Eng. J.* 262, 286–294.
- 1556 Sopaj F., Oturan N., Pinson J., Podvorica F., Oturan M.A., 2016. Effect of the anode
1557 materials on the efficiency of the electro-Fenton process for the mineralization of the
1558 antibiotic sulfamethazine. *Appl. Catal. B: Environ.* 199, 331-341.
- 1559 Srivastava, S., Sinha, R., Roy, D., 2004. Toxicological effects of malachite green. *Aquat.*
1560 *Toxicol.* 66 (3), 319-329.

- 1561 Sun, J., Lu, H., Du, L., Lin, H., Li, H., 2011. Anodic oxidation of anthraquinone dye Alizarin
1562 Red S at Ti/BDD electrodes. *Appl. Surf. Sci.* 257 (15), 6667–6671.
- 1563 Sun, S.P., Li, C.J., Sun, J.H., Shi, S.H., Fan, M.H., Zhou, Q., 2009. Decolorization of an azo
1564 dye Orange G in aqueous solution by Fenton oxidation process: Effect of system
1565 parameters and kinetic study. *J. Hazard. Mater.* 161 (2-3), 1052-1057.
- 1566 Suslick, K.S., 1989. The chemical effects of ultrasound. *Sci. Am.* 260, 80-87.
- 1567 Suteu, D., Bilba, D., 2005. Equilibrium and kinetic study of reactive dye brilliant red HE-3B
1568 adsorption by activated charcoal. *Acta Chim. Slov.* 52, 73–79.
- 1569 Tang, W.Z., Huang, C.P., 1996. 2,4-dichlorophenol oxidation kinetics by Fenton's reagent.
1570 *Environ. Technol.* 17 (12), 1371-1378.
- 1571 Umbuzeiro, G.A., Freeman, H., Warren, S.H., Kummrow, F., Claxton, L.D., 2005.
1572 Mutagenicity evaluation of the commercial product CI Disperse Blue 291 using different
1573 protocols of the Salmonella assay. *Food Chem. Toxicol.* 43 (1), 49-56.
- 1574 Vasudevan, S., Oturan, M.A., 2014. Electrochemistry as cause and cure in water pollution.
1575 An Overview. *Environ. Chem. Lett.* 12(1), 97-108.
- 1576 Venu, D., Gandhimathi, R., Nidheesh, P.V., Ramesh, S.T., 2014. Treatment of stabilized
1577 landfill leachate using peroxicoagulation process. *Sep. Purif. Technol.* 129, 64–70.
- 1578 Venu, D., Gandhimathi, R., Nidheesh, P.V., Ramesh, S.T., 2016. Effect of solution pH on
1579 leachate treatment mechanism of peroxicoagulation process. *J. Hazard. Toxic Radioact.*
1580 *Waste* 20 (3), 06016001.
- 1581 Wang, A., Qu, J., Liu, H., Ru, J., 2008b. Mineralization of an azo dye Acid Red 14 by
1582 photoelectro-Fenton process using an activated carbon fiber cathode. *Appl. Catal. B:*
1583 *Environ.* 84 (3-4), 393–399.
- 1584 Wang, C.T., Chou, W.L., Chung, M.H., Kuo, Y.M., 2010. COD removal from real dyeing
1585 wastewater by electro-Fenton technology using an activated carbon fiber cathode.
1586 *Desalination* 253 (1-3), 129–134.
- 1587 Wang, C-T., Hu, J-L., Chou, W-L., Kuo, Y-M., 2008a. Removal of color from real dyeing
1588 wastewater by Electro-Fenton technology using a three-dimensional graphite cathode. *J.*
1589 *Hazard. Mater.* 152 (2), 601–606.
- 1590 Wang, Q., Jin, T., Hu, Z.X., Zhou, L., Zhou, M.H., 2013. TiO₂-NTs/SnO₂-Sb anode for
1591 efficient electrocatalytic degradation of organic pollutants: Effect of TiO₂-NTs
1592 architecture. *Sep. Purif. Technol.* 102, 180-186.
- 1593 Wang, Q., Lemley, A.T., 2002. Oxidation of diazinon by anodic Fenton treatment. *Water*
1594 *Res.* 36 (13), 3237–3244.
- 1595 Wang, Q., Lemley, A.T., 2003. Oxidative degradation and detoxification of aqueous
1596 carbofuran by membrane anodic Fenton treatment. *J. Hazard. Mater.* B98 (1-3), 241–255.
- 1597 Wang, Z., Qi, J., Feng, Y., Li, K., Li, X., 2014a. Fabrication and electrocatalytic performance
1598 of a novel particle electrode. *Catal. Commun.* 46, 165–168.

- 1599 Wang, Z., Qi, J., Feng, Y., Li, K., Li, X., 2014b. Preparation of catalytic particle electrodes
1600 from steel slag and its performance in a three-dimensional electrochemical oxidation
1601 system. *J. Ind. Eng. Chem.* 20(5), 3672-3677
- 1602 Wells, C.F., Salam, M.A., 1965. Hydrolysis of ferrous ions: A kinetic method for
1603 determination of the Fe(II) species. *Nature* 205, 690–692.
- 1604 Wells, C.F., Salam, M.A., 1968. The effect of pH on the kinetics of the reaction of iron(II)
1605 with hydrogen peroxide in perchlorate media. *J. Chem. Soc. A* 1968, 24–29.
- 1606 Xu, X., Chen, J., Zhang, G., Song, Y., Yang, F., 2014. Homogeneous electro-Fenton
1607 oxidative degradation of reactive brilliant blue using a graphene doped gas-diffusion
1608 cathode. *Int. J. Electrochem. Sci.* 9, 569–579.
- 1609 Yang, W., Zhou, M.H., Cai, J. J., Liang, L., Ren, G.B., 2017. Ultrahigh yield of hydrogen
1610 peroxide on graphite felt cathode modified with electrochemically exfoliated graphene. *J.*
1611 *Mater. Chem. A* 5, 8070–8080.
- 1612 Yao, Y., Zhao, C., Zhao, M., Wang, X., 2013. Electrocatalytic degradation of methylene blue
1613 on PbO₂-ZrO₂ nanocomposite electrodes prepared by pulse electrodeposition. *J. Hazard.*
1614 *Mater.* 263 (2), 726–734.
- 1615 Yavuz, Y., Shahbazi, R., 2012. Anodic oxidation of Reactive Black 5 dye using boron doped
1616 diamond anodes in a bipolar trickle tower reactor. *Sep. Purif. Technol.* 85, 130–136.
- 1617 Yu, F.K., Zhou, M.H., Yu, X.M. 2015. Cost-effective electro-Fenton using modified graphite
1618 felt that dramatically enhanced on H₂O₂ electro-generation without external aeration.
1619 *Electrochim. Acta* 163, 182-189.
- 1620 Yue, L., Wang, K., Guo, J., Yang, J., Luo, X., Lian, J., Wang, L., 2014. Enhanced
1621 electrochemical oxidation of dye wastewater with Fe₂O₃ supported catalyst. *J. Ind. Eng.*
1622 *Chem.* 20 (2), 725–731.
- 1623 Zarei, M., Khataee, A.R., Ordikhani-Seyedlar, R., Fathinia, M., 2010b. Photoelectro-Fenton
1624 combined with photocatalytic process for degradation of an azo dye using supported TiO₂
1625 nanoparticles and carbon nanotube cathode: Neural network modeling. *Electrochim. Acta*
1626 55 (24), 7259–7265.
- 1627 Zarei, M., Niaei, A., Salari, D., Khataee, A., 2010a. Removal of four dyes from aqueous
1628 medium by the peroxi-coagulation method using carbon nanotube–PTFE cathode and
1629 neural network modeling. *J. Electroanal. Chem.* 639 (1-2), 167–174.
- 1630 Zarei, M., Salari, D., Niaei, A., Khataee, A., 2009. Peroxi-coagulation degradation of C.I.
1631 basic yellow 2 based on carbon-PTFE and carbon nanotube-PTFE electrodes as cathode.
1632 *Electrochim. Acta* 54 (26), 6651–6660.
- 1633 Zhang, C., Jiang, Y., Li, Y., Hu, Z., Zhou, L., Zhou, M., 2013. Three-dimensional
1634 electrochemical process for wastewater treatment: A general review. *Chem. Eng. J.* 228,
1635 455–467.

1636 Zhang, C., Zhou, L., Yang, J., Yu, X., Jiang, Y., Zhou, M., 2014. Nanoscale zero-valent
1637 iron/AC as heterogeneous Fenton catalysts in three-dimensional electrode system.
1638 *Environ. Sci. Pollut. Res.* 21, 8398–8405

1639 Zhang, Y., Wang, Y., Angelidaki, I., 2015. Alternate switching between microbial fuel cell
1640 and microbial electrolysis cell operation as a new method to control H₂O₂ level in
1641 Bioelectro-Fenton system. *J. Power Source.* 291,108-116.

1642 Zhao, G., Gao, J., Shi, W., Liu, M., Li, D., 2009. Electrochemical incineration of high
1643 concentration azo dye wastewater on the in situ activated platinum electrode with
1644 sustained microwave radiation. *Chemosphere* 77 (2), 188–193.

1645 Zhao, X., Liu, S., Huang, Y., 2016. Removing organic contaminants by an electro-Fenton
1646 system constructed with graphene cathode. *Toxicol. Environ. Chem.* 98, 530-539

1647 Zhou, L. Zhou, M., Zhang, C., Jiang, Y., Bi, Z.H., Yang, J., 2013. Electro-Fenton degradation
1648 of p-nitrophenol using the anodized graphite felts. *Chem. Eng. J.*, 233, 185-192.

1649 Zhou, L., Zhou, M., Hu, Z., Bi, Z., Serrano, K.G., 2014. Chemically modified graphite felt as
1650 an efficient cathode in electro-Fenton for p-nitrophenol degradation. *Electrochim. Acta*
1651 140, 376-383.

1652 Zhou, M., Yu, Q., Lei, L., Barton, G., 2007. Electro-Fenton method for the removal of methyl
1653 red in an efficient electrochemical system. *Sep. Purif. Technol.* 57 (2), 380–387.

1654 Zhou, M.H., Liu, L., Jiao, Y. L., Wang, Q., Tan, Q.Q., 2011b. Treatment of high-salinity
1655 reverse osmosis concentrate by electrochemical oxidation on BDD and DSA electrodes.
1656 *Desalination* 277, 201-206.

1657 Zhou, M.H., Särkkä H., Sillanpää M.A. 2011a. Comparative experimental study on methyl
1658 orange degradation by electrochemical oxidation on BDD and MMO electrodes. *Sep.*
1659 *Purif. Technol.* 78, 290–297.

1660 Zhu, X., Logan B.E., 2013. Using single-chamber microbial fuel cells as renewable power
1661 sources of electro-Fenton reactors for organic pollutant treatment. *J. Hazard. Mater.*252–
1662 253, 198–203.

1663 Zhu, X., Ni, J., 2009. Simultaneous processes of electricity generation and p-nitrophenol
1664 degradation in a microbial fuel cell. *Electrochem. Commun.* 11 (2), 274–277.

1665